



Oceanographic dataset collected during the 2021 scientific expedition of the Canadian Coast Guard Ship *Amundsen*

Tahiana Ratsimbazafy^{1,3}, Thibaud Dezutter^{1,3}, Amélie Desmarais^{1,3}, Daniel Amirault^{1,3}, Pascal Guillot^{1,2,3}, and Simon Morisset^{1,3}

¹Amundsen Science: 1045 Avenue de la Médecine, Pavillon Alexandre-Vachon, Local 3432, Université Laval, Québec, QC, G1V 0A6, Canada

²Québec-Océan: 1045 Avenue de la Médecine, Pavillon Alexandre-Vachon, Local 2078, Université Laval, Québec, QC, G1V 0A6, Canada

³These authors contributed equally to this work.

Correspondence: Tahiana Ratsimbazafy (tahiana.ratsimbazafy@as.ulaval.ca; amundsen.data@as.ulaval.ca)

Abstract.

Since 2003, the state-of-the-art Canadian Coast Guard Ship (CCGS) research icebreaker *Amundsen* furrows the Canadian Arctic waters to support novel research endeavors and collect oceanographic data. This paper presents the data acquisition, the processing methods and an overview of the data collected during the 2021 expedition as the ship traveled over 30 000 km during 122 days across the Canadian Arctic Ocean, collecting sea surface, atmospheric and seabed underway measurements. A total of 266 casts of a conductivity, temperature and depth profiler mounted on a rosette (CTD-Rosette) were also conducted to monitor the main physical, chemical and biological parameters of the water column. More specifically, the data here presented were collected with the CTD-Rosette across historical sampling transects in Davis Strait, the North Water Polynya (NOW), and Cape Bathurst. A 182 km dedicated survey of Moving Vessel Profiler (MVP), equipped with CTD, transmissometer, dissolved oxygen, fluorescence, sound velocity sensors, was conducted across Hudson Strait. We also present an overview of the data collected by the underway systems (seabed, thermosalinograph and atmospheric). Such data are essential in understanding the impacts of climate warming on the unique environments of the Canadian Arctic Ocean. Amundsen Science supports and promotes easy access and sharing of such valuable data to the scientific community.

1 Introduction

The Canadian Arctic Ocean covers 4 million km², and over 70% of Canada's coastline is within the Arctic region (Niemi et al., 2020). Such a vast area embraces numbers of unique ecosystems, on which it has been challenging to establish a global, strong, and reliable baseline to fully understand the impact of global warming. Over the years, ice camp (Untersteiner et al., 2009; Massicotte et al., 2020), research vessels (such as the CCGS *Amundsen* and the CCGS *Louis Saint-Laurent*), Inuit Knowledge (Weatherhead et al., 2010; Gearheard et al., 2010), and moorings (Armitage et al., 2020; Dezutter et al., 2021; Nadaï et al., 2021) have all been tools used to acquire data and to fill gaps in the Canadian Arctic Ocean knowledge. Meanwhile, satellites and meteorological stations have been providing reliable and rigorous data sets of sea ice and air temperature since



the industrialization period. Previous work showed that the Arctic is warming twice as fast as the rest of the world, and will continue to do so (Serreze et al., 2009; Gulev et al., 2021). In the Canadian Arctic, the summer sea ice extent has been reduced by 7.5% per decade over the 1968-2020 period (Environment and Canada, 2021a) in addition to global thinning (Lindsay and Schweiger, 2015; Meier et al., 2014), while the air temperature has been increasing between 1.5-3.7 °C from the 1948-2018 period over the Arctic land (Environment and Canada, 2021b). The unique ecosystems of the Arctic Ocean, driven by extreme seasonality in light regime and sea ice cover, which dictate the energy transfer through the food web, from micro-algae to large marine mammals (Falk-Petersen et al., 2007) have been directly and indirectly impacted by the drastic loss of sea ice. Changes in timing of biological events (Niemi et al., 2020; Hauser et al., 2017), northern shift of species (Dunmall et al., 2018) (Higdon and Ferguson, 2009) along with increase marine traffic (Halliday et al., 2022; Johnston et al., 2017; Dawson et al., 2018) and pollution (Adams et al., 2021) are all known consequences of the climate change and ice-retreat in the Canadian Arctic.

Since 2003, the CCGS icebreaker *Amundsen* and its leading-edge scientific instrumentation has been monitoring the Canadian Arctic by supporting dozens of large-scale national and international research initiatives from academia, local communities, and the public and private sectors. The CCGS *Amundsen* is the only coast guard ship seasonally dedicated to science, and over 1400 refereed scientific publications and 400 datasets have resulted from the CCGS *Amundsen* expeditions. Hosted at Université Laval, Amundsen Science is the organization responsible for the management of the scientific mandate of the research icebreaker CCGS *Amundsen*. Specifically, Amundsen Science manages the vessel's pool of scientific equipment, coordinates the deployment of the icebreaker for science, and provides logistical, financial, and technical support to user programs. In order to promote and share Canadian Arctic oceanographic data, the objective of this paper is to present an overview of datasets collected by the core instruments managed by Amundsen Science over the 2021 Amundsen scientific expedition. The expedition took place from July 4th to November 3rd and was divided into five Legs¹ taking place in the Labrador Sea, the Baffin Bay, the Canadian Arctic Archipelago, and the Beaufort Sea (Fig. 1). Eight multidisciplinary national and international research programs took part in this annual expedition (Table B1). Research programs objectives are central to the Amundsen expeditions and are supported by Amundsen Science through oceanographic data acquisitions: detailed CTD-Rosette, Moving Vessel Profiler (MVP), underway measurement of sea surface properties with Thermosalinograph (TSG) and atmospheric data, multi-beam echo sounder, single beam echo sounder and sub-bottom profiler datasets were collected during this expedition and are presented in this paper. Information on additional samples collected by the research teams onboard during the 2021 expedition can be obtained by contacting the respective principal investigators (as detailed in Table B1) or by consulting the expedition report (Amundsen Science, 2021b).

¹A Leg is a determined period during which the sampling operations of the ship are scheduled.

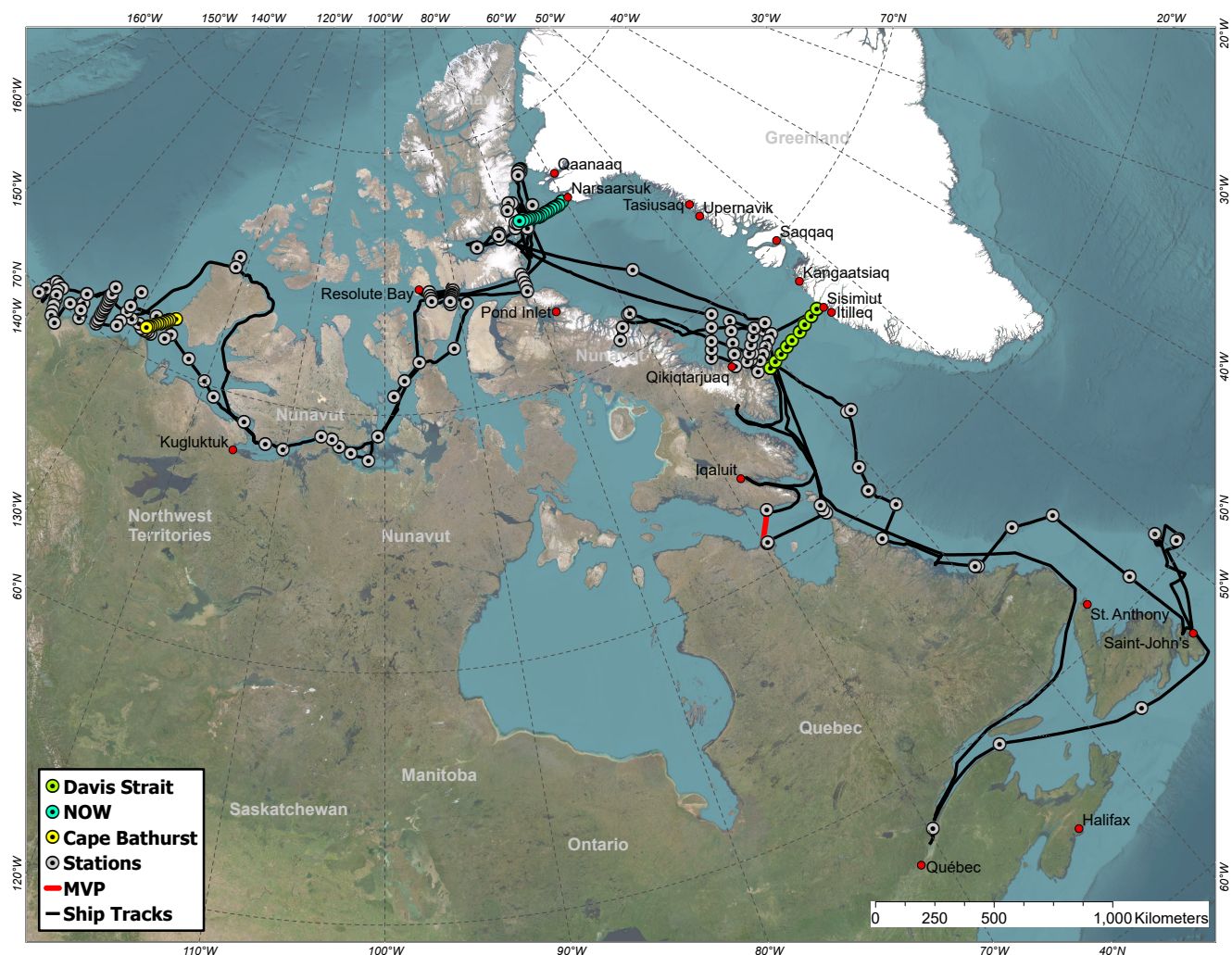


Figure 1. Map of the CCGS *Amundsen* 2021 expedition, including ship track and the locations of CTD-Rosette stations and MVP casts. (©ESRI 2023).

50 1.1 Regional settings

1.1.1 Labrador Sea and Hudson Strait

The Labrador Sea, located between Labrador and Greenland, receives several water currents from different part of the Arctic regions. The Baffin Current from the Baffin Bay brings cold water as well as drifting icebergs and ice islands into the Labrador Sea, acting as corridor for ice transport (Yang et al., 2016; New et al., 2021). Such moving ice blocs was reported by Marko et al. (2014) as presenting risks for activities and operations conducted offshore Newfoundland. Cold waters from Hudson's Bay Current circulates through Hudson Strait to the Labrador Sea where it joins warm sub-arctic water from the North Atlantic

55



Current (McGeehan and Maslowski, 2012; Yang et al., 2016) and feeds the source of water mass formation in the Labrador and Irminger Seas (Kieke and Yashayaev, 2015).

60 Exchanges of carbon dioxide, oxygen, and heat between the deep ocean and the atmosphere have been reported by Clarke and Coote (1988); Azetsu-Scott et al. (2003); DeGrandpre et al. (2006); Körtzinger et al. (2008); Yashayaev and Seidov (2015) to occur in Labrador Sea area. They arise from deep ocean convection process during winter when heat losses occurs and cold waters sink to greater dept, produces the Labrador Sea Water (McCartney, 1992; Kieke et al., 2009), and allows the possibility of exchange between the intermediate and deep waters with the surface water and the atmosphere (Kieke et al., 2009).

65 Such complexity of system processes occurring in the Labrador Sea demonstrate how important is the gathering of scientific knowledge as a guidance for different decision makers to monitor risks associated to different activities such as exploration and exploitation of oil and gas in order to keep the safety of marine ecosystem in the region.

1.1.2 Baffin Bay

70 Located between the Baffin Island and Greenland, Baffin Bay is connected to the Lincoln Sea through Nare Strait one of the pathways of sea ice transport from the Arctic Ocean Sea into Baffin Bay (Kwok, 2005). Lancaster and Jones Sound are considered as corridor as well, connecting Baffin Bay to the Arctic Ocean allowing ices and fresher waters being transported downstream to Davis Strait and the Labrador Sea (Tang et al., 2004). Despite it's location in high latitude, Baffin Bay is under the influence of the northward West Greenland Current (WGC), bringing warm and salty waters and exchanges heat, salt, and ice with the southward Baffin Island Current in an anti-clockwise circulation (Arctic Monitoring and Assessment Programme (AMAP), 2018).

75 In Nares Strait, between Ellesmere Island and Greenland, ice arches typically form each winter at both its northern and southern end (Moore et al., 2021). The formation of an ice arch in Nares Strait and the resulting cessation of ice transport, the input of warm and salty Atlantic water from the West Greenland current, and upwelling of warmer waters, all contribute to the formation of the North Water (NOW) Polynya, a year-round expanse of open waters in Smith Sound and northern Baffin Bay which is the largest and most productive of its kind (Melling et al., 2001; Moore et al., 2019). The thinning of the Arctic sea-ice 80 is negatively affecting the stability of these ice arches, which results in an acceleration in the loss of multi-year ice from the Arctic and could impact the NOW polynya ecosystem (Moore et al., 2021; Kwok et al., 2010; Moore et al., 2019).

85 Glaciers, icecaps, and icefields of the Canadian Arctic and Greenland also contribute to the freshwater input in Baffin Bay via their runoff through fjords, rivers, and calving (Bamber et al., 2018). Some icefields, such as the Manson icefield (southeast Ellesmere Island, Canada) directly connect with Northern Baffin Bay. In the Canadian Arctic, the Manson icefield has the highest concentration of surging glaciers, characterized by surging periods and variable glacier and freshwater flow (Copland et al., 2003).

During the 2021 Arctic expedition, the CCGS *Amundsen* visited Baffin Bay and Northern Baffin Bay for scientific sampling activities to monitor seawater physics, chemistry nutrients, contaminants, and the biodiversity present along precise historical transects, glacier fronts and Baffin Island fjords.



90 1.1.3 Canadian Arctic Archipelago (CAA)

The CAA covers several islands and channels between Banks Island in the west and Baffin and Ellesmere Islands in the east. This area is characterized by the mixing of Pacific, Atlantic and Arctic-originated waters, a strong year-to-year variability in oceanographic and biological processes and changing sea ice conditions (Michel et al., 2006; Pizzolato et al., 2014). Over the last decades, marine transport in the region has increased due to the easing in shipping navigability driven by reductions in the extent, thickness and age of sea ice (Kwok et al., 2009). As the CAA could become the larger outlet for Arctic Ocean ice area loss (Howell and Brady, 2019), risk of collision resulting in potential Arctic oil spills are high (Helle et al., 2020). Arctic Council's Working Group on the Protection of the Arctic Marine Environment (PAME) (2020) indicated the importance of collecting bathymetric and sub-bottom data for seafloor mapping, identifying potential geohazards and obstacle to a safe navigation in the newly open Arctic.

100 Collecting bathymetric data for seafloor mapping is a challenging task for a large area with limited access such as the Arctic. An earlier version of digital bathymetric data, International Bathymetric Chart of the Arctic Ocean (IBCAO) was first introduced by Jakobsson et al. (2000) at AGU conference on 1999. The data was part of the declassified historic sounding collections from the United State and the British submarines between 1957 to 1988. Several updates has been made since using models and new data from different sources Jakobsson et al. (2008, 2012).

105 During the expedition year 2021, the CCGS *Amundsen* collected echo-sounding data at Smith Bay, Ellsmere Island. Descriptions of instruments for seabed data acquisition and samples from the seabed mapping are presented in Sect. 2.3.3 and Sect. 3.5 respectively.

1.1.4 Beaufort Sea

Recently, important changes on sea ice has been reported in both Beaufort Sea and the Mackenzie Shelf region of the Arctic Ocean (Comiso, 2002; Galley et al., 2016; Mudryk et al., 2018). The first year ice is becoming more common in the area due to increased transport of old ice away from the regional peripheral Arctic seas (Nghiem et al., 2007; Ogi et al., 2008; Hutchings and Rigor, 2012). The Beaufort Sea shelves are mostly influenced by input sediment-rich from the Mackenzie River

The Beaufort Sea is characterized by a broad shelf onto which the Mackenzie River indicated in (Carson et al., 1998) as the most sediment-rich river in the Arctic by then with 130×10^6 tonnes/yr, carries a large and highly seasonally variable amounts of freshwater (Carmack and Macdonald, 2002).

115 Along the Mackenzie Shelf stretches the highly productive Cape Bathurst polynya, the third biggest expanse of open water that has existed year-round (Arrigo and van Dijken, 2004). This ecosystem is also exceptional since it provides habitat for some of the highest densities of birds and marine mammals in the Arctic (Harwood and Stirling, 1992; Dickson and Gilchrist, 2002), although climate change-induced stress and anthropogenic activities are putting and increasing pressure on the ecosystem (Hoover et al., 2021).

120 Since 2002, extensive multidisciplinary research programs have been conducted in the Beaufort Sea area from the CCGS *Amundsen* through international overwintering research programs including Canadian Arctic Shelf Exchange Study (CASES)



in 2003-2004 and Circumpolar Flaw Lead (CFL) Study in 2007-2008. Environmental and oceanographic research activities were also conducted in the offshore region of the Mackenzie Shelf, shelf slope and Beaufort Sea within the framework of the Beaufort Regional Environmental Assessment program (BREA).

2 Data acquisition, processing and quality control

Data collected and the subsequent methods applied to ensure quality assurance and quality control (QAQC) are presented in the following section. Unless specified otherwise, all processing scripts are publicly available at Guillot et al. (2022).

2.1 CTD-Rosette profiler

The CCGS *Amundsen* is equipped with a Sea-Bird Scientific© SBE 911plus CTD (SBE 9plus CTD unit combined with SBE 11plus V2 deck unit) mounted on a SBE 32 carousel water sampler with twenty-four 12L Niskin bottles, model 110BES by Ocean Test Equipment (Appendix C2). Along with the basic SBE CTD sensors (temperature, conductivity, pressure, dissolved oxygen), the SBE 9plus supports several auxiliary sensors (nitrate, transmissometer, colored dissolved organic matter, fluorescence, photosynthetically active radiation (PAR)). Conductivity, temperature and fluorescence sensors are doubled to ensure data redundancy and reliability. A surface PAR (SPAR) sensor is also installed at the top of the bridge between 10-15 m from the sea surface and provides reference values. The main sensors are factory calibrated every year before the cruise period and are post-calibrated after the cruises that allows to detect any problems such as drift. An independent LADCP (lowered acoustic doppler current profiler) is also mounted to the frame in order to measure the horizontal current velocities throughout the water column. The LADCP is a Teledyne 300kHz instrument and is looking downward. It is set up to record data with 8 m bin size, one ping per second and zero blanking. Technical specifications related to each sensor mounted on the rosette are summarized in Table 1.

The water samples collected with the CTD-Rosette are used by multiple scientific programs (Table B1 in Appendix) and by Amundsen Science for data validation. The conductivity sensors are compared with salinity water samples analyzed with a 8400B Guildline salinometer. The dissolved oxygen sensor is validated with water samples analyzed via the Winkler method. Other sensors such as the Suna nitrate sensor or the Seapoint fluorescence sensors are validated with water samples if they are analyzed and available from other scientific teams.

The Fig. 2 depicts the temperature and salinity anomalies recorded by the dual sensor system. Good agreement is obvious between the two temperature sensors. However, the salinity sensor presents a slight and continuous drift by the end of Leg 5. The comparison with the water samples allowed to determine the faulty sensor.

The CTD data are processed using the Seabird data processing software and using the recommended processing module sequences. The QAQC procedure is mainly based on the Global Temperature and Salinity Profile Program (GTSP) Commission et al. (2010) quality control tests. Additional tests including pump status checking or downcast versus upcast comparisons or doubled sensors comparisons (temperature and salinity) are applied as well. Moreover, the main sensors such as temperature, conductivity and dissolved oxygen are factory post-calibrated to detect potential issues.



Table 1. Instruments and specifications of the CTD-Rosette deployed during the 2021 expedition of the CCGS *Amundsen*.

Instrument	Company	Variables	Specifications
SBE 3plus	Sea-Bird Scientific	Temperature	Resolution at 24 Hz: 0.0003 °C Initial accuracy: ± 0.001 °C
SBE 4	Sea-Bird Scientific	Conductivity	Resolution at 24 Hz: 0.00004 Sm ⁻¹ Initial accuracy: 0.0003 Sm ⁻¹
Deep Suna	Sea-Bird Scientific	Nitrate	Range: 3000 μM Resolution: ±0.5 μM Accuracy: ±2 μM
SBE 43	Sea-Bird Scientific	Dissolved Oxygen	Range: 120 % of surface saturation Accuracy: 2 % of saturation
FLCDRTD	Sea-Bird Scientific (Wetlabs)	CDOM	Range: 0 to 500 ppb Sensitivity: 0.09 ppb
C-Star	Sea-Bird Scientific (WetLabs)	Beam Transmittance	Optical pathlength: 25 cm Wavelength: 25 657 nm Sensitivity: 1.25 mV Response time: 0.167 s
Digiquartz [®] pressure	Paroscientific, Inc.	Pressure	Range: 0-6800 m Resolution at 24 Hz: 0.001 % Initial accuracy: 0.015 %
SCF	SeaPoint Sensors, Inc.	Fluorescence	Range: 0-15 μgL ⁻¹ * Sensitivity: 0.33 Vμg ⁻¹ L Minimum Detectable Level: 0.02 μgL ⁻¹
QCP-2350	Biospherical Instrument Inc.	PAR (Irradiance)	Spectrum: 400-700nm PAR range: 0-5000 μEinsteins m ⁻² s ⁻¹
QCR-2200	Biospherical Instrument Inc.	SPAR (Surface Irradiance)	Spectrum: 400-700nm PAR range: 0-5000 μEinsteins m ⁻² s ⁻¹
LADCP	Teledyne RDI Workhorse	Current velocities	Frequency at 300 kHz

* The SCF can be used in four sensibility and range configurations. The 15 μgL⁻¹ range configuration was used for all casts of the 2021 expedition. For QCP-2350 specifications, see Biospherical Instruments Inc. (2014). Most QCR specifications are known to be identical with those of QCP sensors.

155 The conservative temperature and absolute salinity presented in this paper are calculated using the Gibbs SeaWater (GSW) Oceanographic Toolbox (McDougall and Barker, 2011), based on the thermodynamic equation of seawater 2010 (TEOS-10) (IOC et al., 2010).

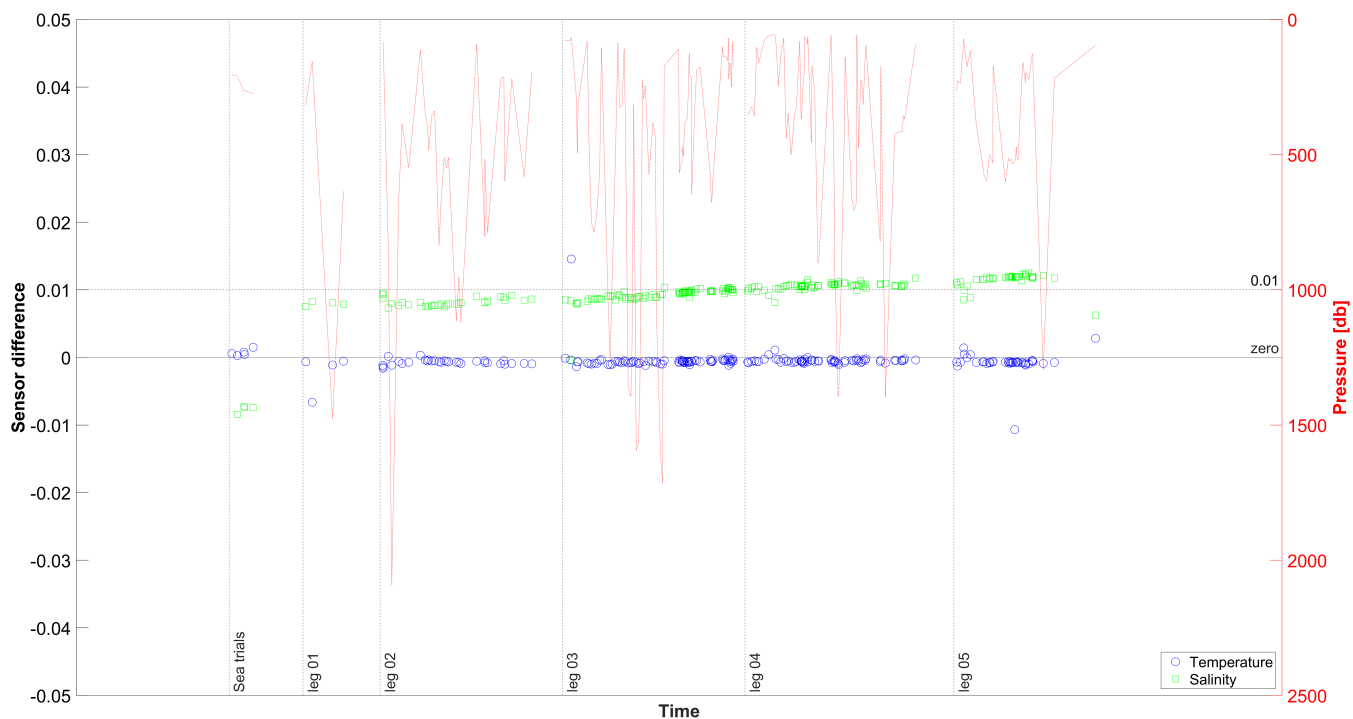


Figure 2. CTD anomaly evolution between the dual Sea-Bird Conductivity (green) and Temperature (blue) sensors along the sea-trial and the 5 Legs. Both Salinity and Temperature were used to calculate the anomaly. They are extracted from the highest pressure values (red) from each profiles (last quarter of the pressure range).

2.2 Moving Vessel Profiler[®]

The AML Oceanographic Moving Vessel Profiler[®] (MVP300) is part of the central pool of instruments operated by Amundsen
160 Science on the CCGS *Amundsen*. With its capability of supporting both shallow and deep-water data sets collection, the MVP's
primary function is to allow accurate data collection of all the water column without the need to stop the vessel. The system
includes a computer-controlled smart winch and deployment system that allows continuous up and down casts of the free fall
fish. The fish is equipped with seven sensors to record oceanographic data along a transect of vertical dives of the fish. The
installed probes include temperature, conductivity, pressure, sound velocity, dissolved oxygen, fluorescence, and transmittance
165 sensors. Technical specifications related to the sensors mounted on the MVP are presented in the Table 2.

MVP data processing is conducted using a MATLAB[®] in-house processing script developed by Amundsen Science. Processing
steps are sequentially applied on each cast of a given MVP transect and include the conversion of analog inputs into
digital inputs, the flagging of out of range and spiking values and the average over 1m depth.

Derived parameters are also calculated (e.g.: salinity, sound velocity, etc.) and manual data check is conducted to ensure the
170 quality of the data. The final processed data are saved in text-based format. More details are available in the MVP processing
report (Amundsen Science (2021a)).



Table 2. Instrumentation and specifications of the MVP during the 2021 expedition

Instrument	Company	Variables	Specifications
Micro CTD	AML	Temperature	Range: -2-32 °C Initial Accuracy: 0.005 °C Resolution: 0.001 °C
		Conductivity	Range: 2-70 mScm ⁻¹ Initial Accuracy: 0.01 mScm ⁻¹ Resolution: 0.0015 mScm ⁻¹
		Pressure	Range: 0-600 bar Initial Accuracy: 0.05 %FS Resolution: 0.1 dbar
Micro SV	AML	Sound velocity	Range: 1375-1600 ms ⁻¹ Initial Accuracy: 0.05 ms ⁻¹ Resolution: 0.01 ms ⁻¹
		Pressure	Range: 0-600 bar Initial Accuracy : 0.05 %FS Resolution: 0.1 dbar
Rinko III	JFE Alec	Dissolved Oxygen	Range: 0-100 % Response time: 0.9 s (90%) Drift: 5 % per month
ECOFLO	Sea-bird (WetLabs)	Fluorescence	Range: 0-125 µgL ⁻¹ Sensitivity: 0.062 µgL ⁻¹ Wavelength: 470 and 695 nm
C-Star Transmissometer	Sea-Bird (WetLabs)	Beam Transmittance	Optical pathlength: 25 cm Wavelength: 657 nm Sensitivity: 1.25 mV Response time: 0.167 s



2.3 Underway systems

2.3.1 Thermosalinograph (TSG)

The CCGS *Amundsen* is equipped with a continuous underway seawater sampling system including a ThermoSalinoGraph (TSG) for temperature and conductivity measurements coupled with a fluorometer, a sound velocity sensor and an additional temperature sensor. A 20 mesh size strainer is placed at the beginning of the line to filter the surface seawater, which circulates under the ship to reach the TSG installation under the vessel's deck before entering the water line. Technical specifications related to the sensors included on the TSG are presented in Table 3. Geolocations (latitude, longitude), dates and times of the recording are presented alongside the Practical Salinity, and Sea Water Temperature. Other variables related to the ship (vessel speed [kn], water flow rate [L/min]) are presented in the dataset as well.

The configuration of the TSG is shown in appendix C. Data processing is conducted using the MATLAB® in house processing script (available at Sect. 6), and requires the use of navigation data, atmospheric data, seawater surface salinity samples from the TSG (analyzed with Guildline salinometer) and CTD-Rosette data for inter-comparison and correction. Processing steps include the flagging of out of range values, the averaging over 1 minutes and intercomparison and correction with collocated data from the CTD-Rosette and in-situ samples is made. The final processed data are saved in text-based format. More details are available in the TSG processing report published with the dataset (Science (2021c)).

Table 3. Instrumentation and specifications of the Thermosalinograph (TSG) during the 2021 expedition (Morisset, 2021)

Instrument	Company	Variables	Specifications
SBE 45	Sea Bird	Temperature	Range: -5-35 °C Initial Accuracy: 0.002 °C Resolution: 0.0001 °C
		Conductivity	Range: 0-7 Sm ⁻¹ Initial Accuracy: 0.0003 Sm ⁻¹ Resolution: 0.00001 Sm ⁻¹
		Salinity (derived value)	Initial Accuracy: 0.005 psu Resolution: 0.0002 psu
SBE 38	Sea Bird	Temperature	Range: -5-35 °C Initial Accuracy: 0.001 °C Resolution: 0.00025 °C
WETStar	Wetlabs	Fluorescence	Range: 0.03-75 µgL ⁻¹ Initial Accuracy: 0.03 µgL ⁻¹
Micro X PISO	AML	Sound velocity	Range: 1375-1625 ms ⁻¹ Initial Accuracy: 0.025 ms ⁻¹ Resolution: 0.001 ms ⁻¹



Data quality assessment for the practical salinity is shown on Figure 3. Uncertainty value is roughly equal to 0.01 PSU while the bias stays constant when compared to the result from the CTD Rosette. To be consistent of the data sets presented in the present paper, the Absolute Salinity is presented instead of the Practical Salinity. The Absolute Salinity was calculated using the new thermodynamique equation of seawater (TEOS-10) (McDougall et al., 2009) within the Gibbs-SeaWater (GSW) toolbox by McDougall and Barker (2011).

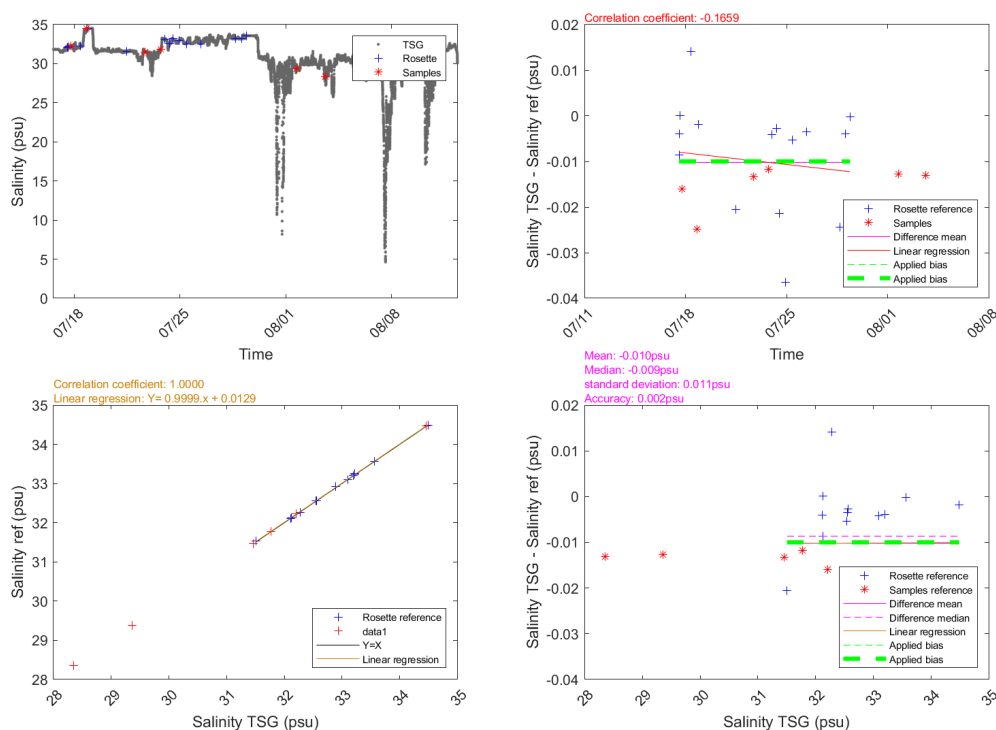


Figure 3. Practical Salinity quality assessment. (Morisset, 2021)

2.3.2 Atmospheric data

The CCGS *Amundsen* is part of the worldwide Voluntary Observing Ship (VOS) scheme, led by the World Meteorological Organization (WMO). As part of this program, an Automated Voluntary Observing Ship system (AVOS) is installed by Environment and Climate Change Canada (ECCC) on the ship to record continuous data on atmospheric pressure, wind speed, wind direction, air temperature and humidity. Amundsen Science retrieves and processes the available AVOS data and add them to the available pool of data. Data processing is conducted using a MATLAB® in house processing script (available at Sect. 6) and includes flagging out of range values, environmental corrections (e.g.: wind speed, vessel pitch and roll, shadow, etc), averaging data over 2 minutes and manual checks.



200 Processed data are saved in text-based format (one file for each leg). More details are provided in the AVOS processing report (Science (2021a)).

Table 4. Instruments and specifications of the AVOS underway system

Instrument	Company	Variable	Specifications
Digital Barometer -PTB-210	Vaisala	Atmospheric pressure	Range: 50-1100 hPa Accuracy: 0.35 hPa Resolution: 0.1 hPa
Anemometer - 05103	Young R.M.	Wind speed	Range: 0-100 m s ⁻¹ Initial accuracy: 0.3 ms ⁻¹
		Wind direction	Range: 0-360° Initial accuracy: 3°
MP101	Rotronic Meteorological	Air temperature	Range: -40-60°C Initial accuracy: 0.2°C
		Humidity	Range: 0-100% RH Initial accuracy: 1% RH
SPAR - QCR2200	Biospherical Instruments	Photosynthetically active radiation	Range: 0-5000 μEm ⁻² s ⁻¹ Initial accuracy: 1.7 μEm ⁻² s ⁻¹

2.3.3 Seabed Data Acquisition Instruments

During the 2021 mission, the CCGS *Amundsen* was equipped with a Kongsberg® multibeam echo sounder (EM302), and a Knudsen 3260 sub-bottom profiler to acquire dedicated and underway seabed data. The seabed data acquisition systems opportunistically operate throughout the entirety of each scientific expedition. Seabed mapping relies on analyzing acoustic pulses propagated and received by echo sounders to generate georeferenced models of the seabed. The bathymetry consists of three-dimensional topographic point clouds of the seafloor, whereas sub-bottom consists of vertical profiles of strata layers below the seafloor. Arctic seabed mapping supports a wide range of research (habitat mapping, geology, paleoclimatology, glacial history, archaeology, geohazards, geopolitics, and more) and provides ships with needed information to navigate safely.

210 The CCGS *Amundsen*'s EM302, upgraded to the Kongsberg® EM304 MKI in summer 2022, is a 30kHz system capable of acquiring data in 10-8000 m water depth. The multibeam echo sounder integrates Global Navigation Satellite System and inertial measurement unit data from the Applanix POSMV V4 to georeference generated soundings. The Kongsberg Seafloor Information System (SIS) acquisition software retrieves acquired EM302 data from the system's processing unit and optimizes data quality using various parameters and tools applied by onboard technicians. The following procedures are used to process

215 raw multibeam data and convert it into deliverable products:



- Sound velocity profiles are derived from each CTD-Rosette station and applied to the multibeam during acquisition. Onboard operators integrate real-time sound velocity measurements at the transducer face, and conduct quality assurance of each cast. If CTD-Rosette casts are sparse and require long transits between deployments, synthetic sound velocity profiles are applied using the 2009 and 2013 World Ocean Atlas Models (WOA09 and WOA13).
- 220 – Raw EM302 data are imported to CARIS HIPS and SIPS[®], where data is georeferenced to absolute positions, depths are converted to reference the Mean Sea Level (MSL) Datum using the WebTide Tidal Solution Model[®], and total propagated uncertainty is calculated.
- Operators revise data in the HIPS and SIPS[®] 2D and 3D Subeditor tool and manually reject erroneous data points from the data set.
- 225 – Cleaned bathymetry data is exported to raster surfaces, catalogued, and distributed.

Processed data are saved in raster format and publicly available through a multitude of sources indicated on Amundsen Science's website Science (2023).

3 Data overview

3.1 CTD-Rosette

230 During the 2021 expedition, Amundsen Science deployed the CTD-Rosette on 266 occasions, producing respectively 4, 35, 83, 103 and 41 casts during legs 1 to 5 spanning across the Canadian and Greenlandic Arctic, from the coast of Labrador to Beaufort Sea (Figure 1). Historical CTD transects were visited during the 2021 expedition and three were selected to present an overview of the CTD data collected during this expedition in Davis Strait, northern Baffin Bay (NOW), Cape Bathurst. These transects are called *historical*, as they were visited multiple times since 2003 by the CCGS *Amundsen*. Note that the
235 Davis Strait transect has only been visited since 2018, but is intended to be visited yearly from now on. For each transect, interpolated values of Conservative temperature (CT), the dissolved oxygen (DO) and absolute salinity (AS) are presented. The seafloor data represented in the following figures are retrieved from echo sounder depth data along the ship track. TS diagrams compiling all the profile from the transect are also presented for each transect in order to describe water mass of the area.

240 3.1.1 Davis Strait

Nine stations were sampled along the Davis Strait between August 17th-20th 2021 (Table A1). A clear distinction between water properties of the eastern and western part of Davis Strait was observed (Fig.4). The Davis Strait water masses have been extensively described in the past and the four main water masses of the region were observed (Fig. 5) during the sampling from the CCGS *Amundsen* (Tang et al., 2004; Curry et al., 2011; Lehmann et al., 2019; Punshon et al., 2014). The West
245 Greenland Slope Current (WGSC) water mass is characterized by discontinued layers of highest salinity (up to 34.5 g/kg), warm



temperature (2.4°C) and relatively poor DO_2 concentration ($250\text{--}300\ \mu\text{M}$). This water mass is present along the Greenland slope between 100–700 dbar. The water mass present over the Greenland Shelf, is characterized by the highest temperatures recorded along the transect (up to 6.5°C), relatively rich in oxygen ($300\text{--}340\ \mu\text{M}$) and fresher waters (up to $34.1\ \text{g/kg}$). Over the western side of the Strait, Baffin Island Current (BIC) water mass, can be observed in the top 200 dbar. This water mass is characterized by the lowest salinity recorded in this transect (between $30\text{--}33.7\ \text{g/kg}$) and highest DO_2 concentration ($420\ \mu\text{M}$) in the surface layers, which extends over the Greenland slope. Coldest temperature are also observed in the BIC (-1.5°C), between 50–200 dbar. Finally, the Atlantic derived waters of the western part of Davis Strait are characterized by relatively warm ($\leq 2^{\circ}\text{C}$), oxygen depleted and relatively salty ($> 33.7\ \text{g/kg}$), ($< 280\ \mu\text{M}$) waters below 300 dbar (Fig. 9b, Fig. 4c, and Fig.4d). Water masses distinctions in Fig. 5 were derived from Curry et al. (2011); Tang et al. (2004).

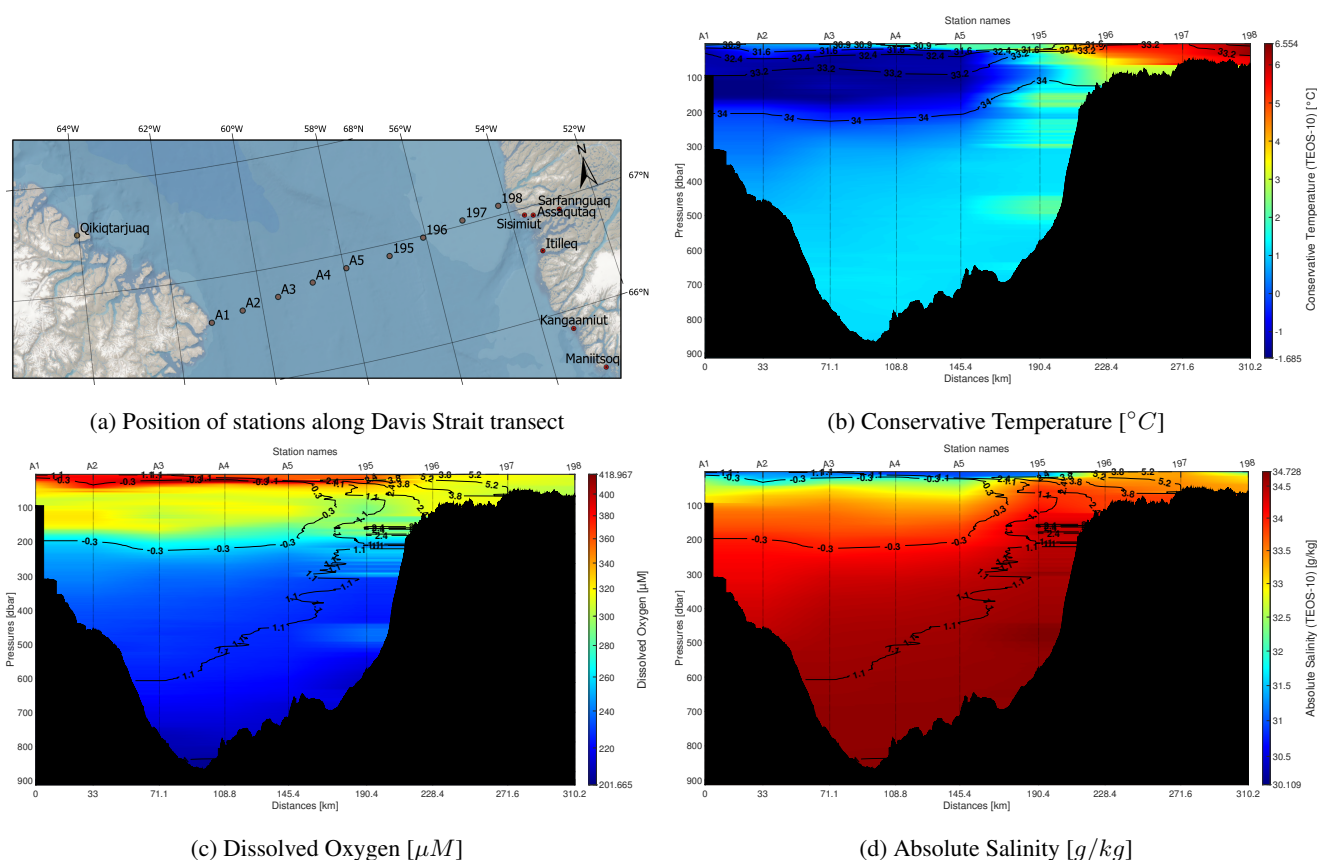


Figure 4. Davis Strait transect profiles during leg 3 of 2021 expedition. Isolines represents conservative temperature (isotherms, in $^{\circ}\text{C}$).

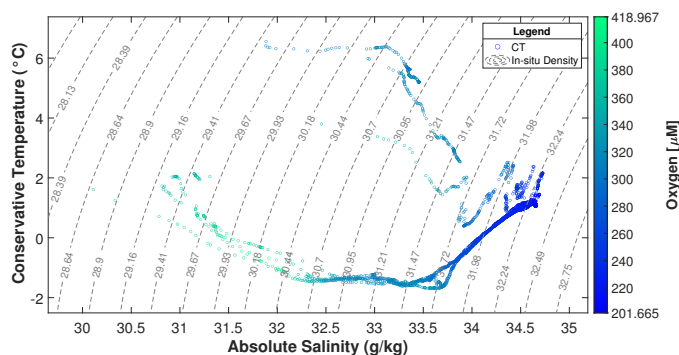
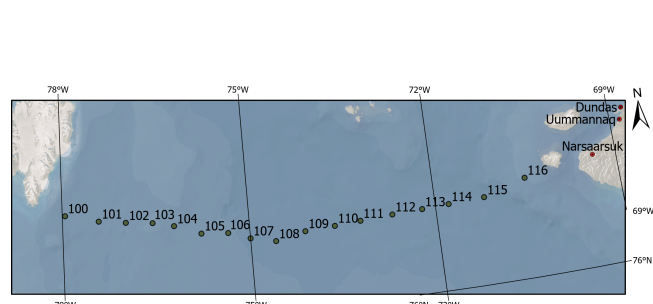


Figure 5. TS Diagram represented by Absolute Salinity (AS), and Conservative Temperature (CT). The isolines are the In-Situ Density calculated with AS and CT.

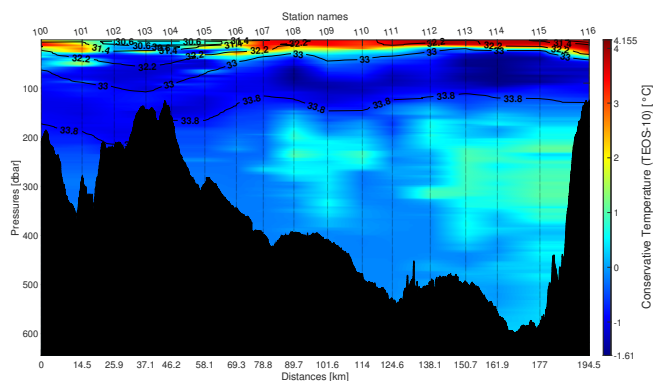
255 3.1.2 North Water Polynia (NOW)

Seventeen stations were sampled along the NOW Transect between August 31st and September 3rd (Table A2). Figure 6a, 6b, 6c, 6d show position of the different CTD-Rosette casts, interpolated values of conservative temperature (CT), dissolved oxygen (DO) and absolute salinity (AS) respectively through the water column at each stations along the NOW transect. As stated by (Bâcle et al., 2002; Lobb et al., 2003), the West Greenland Current (WGS) brings the warm and salty Atlantic waters in the region between 200 and 400 dbar. This water mass can be observed in Fig. 6 by two distinctive cells between stations 107 and 111 and between station 111 and 116, where the maximum value of AS (34.5 g/kg) and lowest value of DO concentration ($< 250 \mu M$) of the transect are located. Relatively warm temperature of $1^\circ C$ also define the water mass. This water mass is trapped under a cold halocline observed between 50-150 dbar Bâcle et al. (2002); Lobb et al. (2003). Based on Figure 6d, this layer is characterized by absolute salinity values ranging from 33-33.8 g/kg, temperature colder than $0.7^\circ C$ and waters relatively rich in DO, ranging from 295-340 μM . A warm, fresh and DO rich (max 400 μM) polar mixed layer (PML) is observed from surface at roughly 75 dbar along the transect. Between stations 101 and 107 a colder and fresher surface layer is observed over the ridge (Fig. 6d). A thin rich DO layer can be observed within the PML around 30 dbar and is extended up to 100 dbar over the ridge (stations 101 to 105). This water is mostly coming for the north by Smith Sound and from the West by Jones Sound and has been warmed up during summer (Bâcle et al., 2002; Lobb et al., 2003).

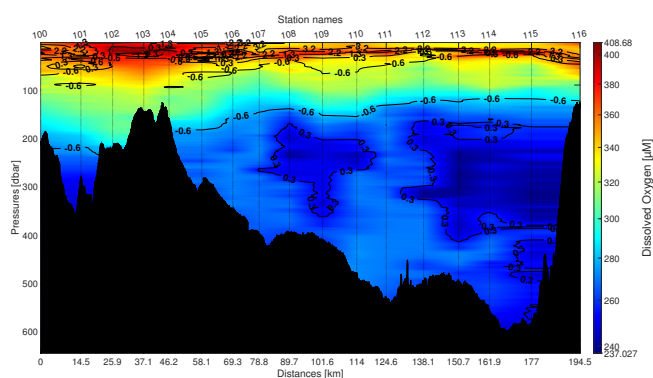
270 All CTD casts of NOW transect are plotted in TS-diagram (Figure 7). Different water masses signatures showcased through the diagram are derived from (Bâcle et al., 2002). Along the transect, two water masses defined by two sets of conservative temperature, on the left side of the figure. They correspond to density values less than $29.47 \text{ kg}\cdot\text{m}^{-3}$. Mixture of waters are observable in the layer with density values between $29.47 \text{ kg}\cdot\text{m}^{-3}$ and $31.4 \text{ kg}\cdot\text{m}^{-3}$.



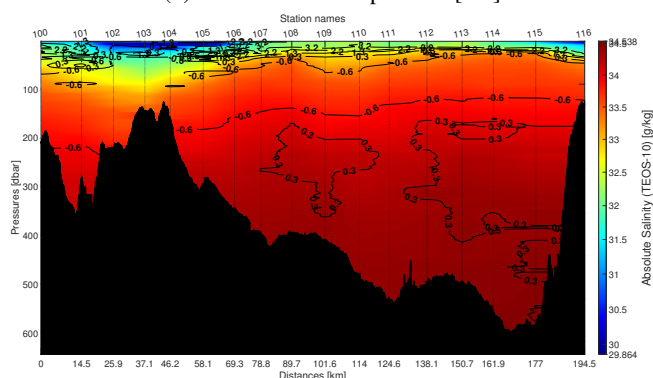
(a) Position of stations along the NOW transect



(b) Conservative Temperature [$^{\circ}\text{C}$]



(c) Dissolved Oxygen [μM]



(d) Absolute Salinity [g/kg]

Figure 6. NOW transect profiles during leg 3 of 2021 expedition. Isolines represents conservative temperature (isotherms, in $^{\circ}\text{C}$).

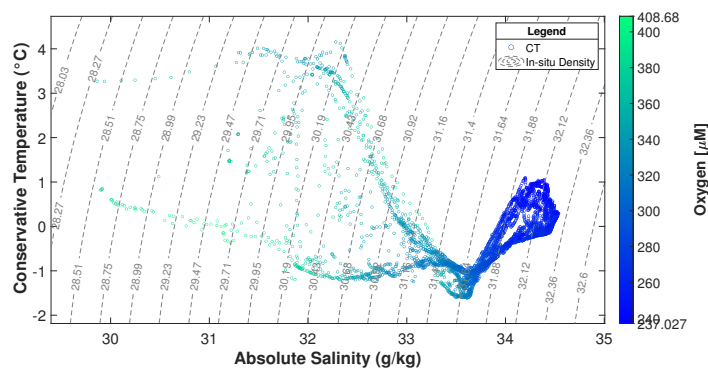


Figure 7. NOW TS Diagram. The isolines are the in-situ density calculated with absolute salinity and conservative temperature.



3.1.3 Cape Bathurst

275 Twelve stations were sampled from Sachs Harbour towards Cape Bathurst on September 18th- 19th (Table A3). The transect
crosses over a major gateway of Arctic water mass exchange. TS diagram regrouping all casts along the Cape Bathurst transect
displays similar profiles than previously discussed by Lansard et al. (2012); Simpson et al. (2008) in the southeastern Beaufort
Sea region 8. In September 2021, 3 major water masses can be observed. The polar mixed layer (PML) is observed from
surface to 25-50 dbar with a stable low salinity (27-30 g/kg), while temperature is much more contrasted (ranging from -1-3.5
280 °C). The surface layer become thinner as we go toward Cap Bathurst, from station 409 to station 420. Under the PML lays
the halocline waters between 50-200 dbar, originated from the Pacific. This water mass shows increasing salinity from 31 to
34 g/kg toward the base of the layer. The coldest temperatures are recorded in the halocline layer (-1.5 °C) and DO of 270
 μM . Finally, the Atlantic Water lays below 250 dbar with a salinity around 34 g/kg, temperature of 0.5 °C and a minimum DO
concentration of 225 μM . A possible upwelling can be observed at station 411 where there is intrusion of deep high salinity
285 water in the halocline layer. Upwelling were already observed in the region by Williams and Carmack (2008). Conservative
temperature shows a pattern of inversion, as values are higher at the surface at station 409 and at the Station 415 to 420, and
at pressures deeper than 150 dbar (Fig.9). The Amundsen has been sampling in the Cape Bathurst area 12 times since 2003,
which produce an extensive dataset for interannual comparison studies. Recently, Massicotte et al. (2021) have compile and
standardize the collected datasets from the 2009 MALINA expedition in the Beaufort Sea, in order facilitate their reuse. Such
290 dataset can be compare to the ones collected by the Amundsen during the 2021 expedition.

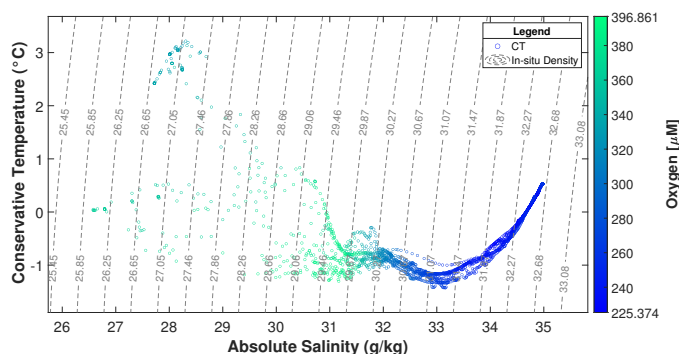


Figure 8. Cape Bathurst transect TS diagram. The isolines are the in situ density values calculated with AS and CT.

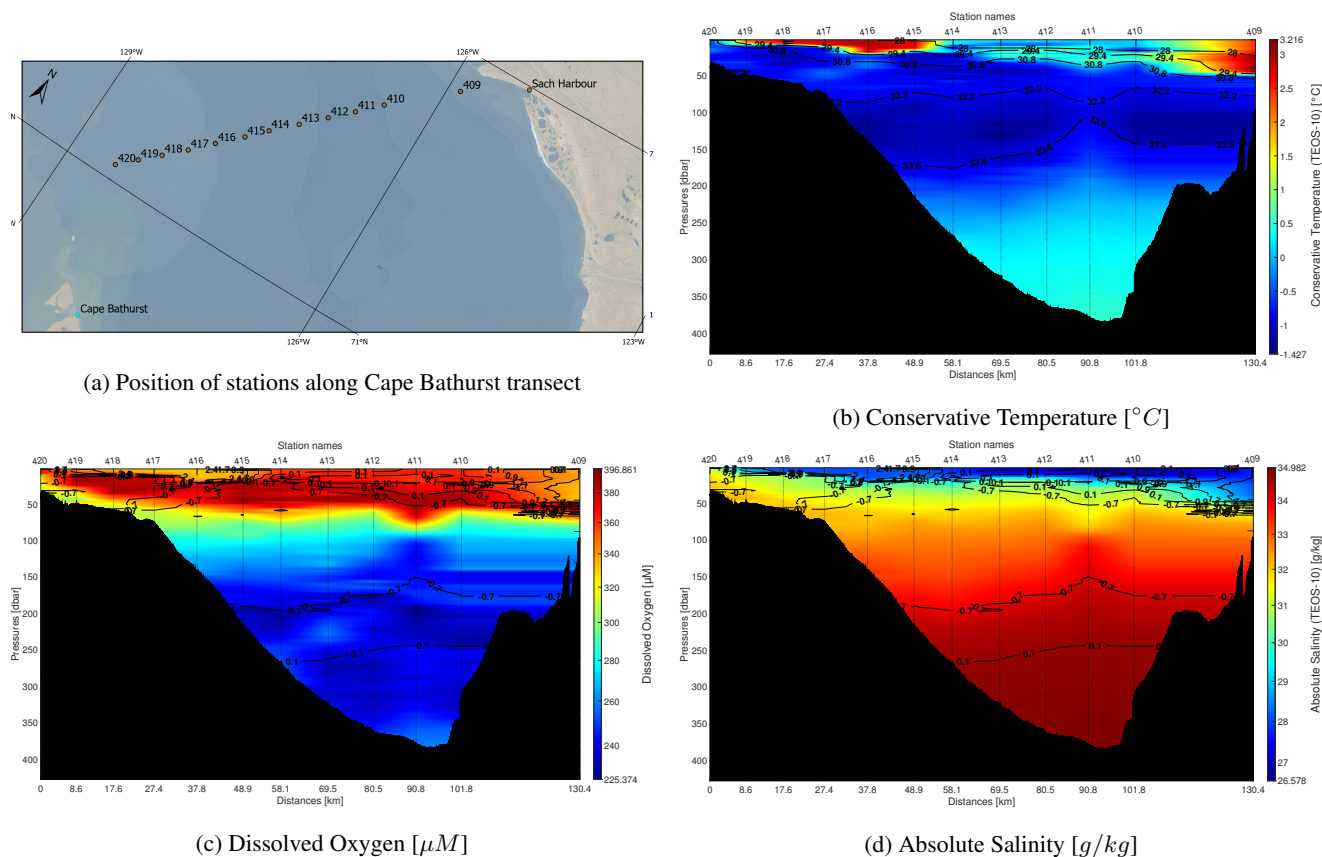
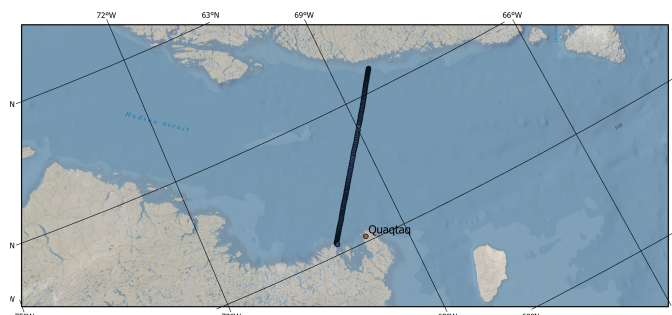


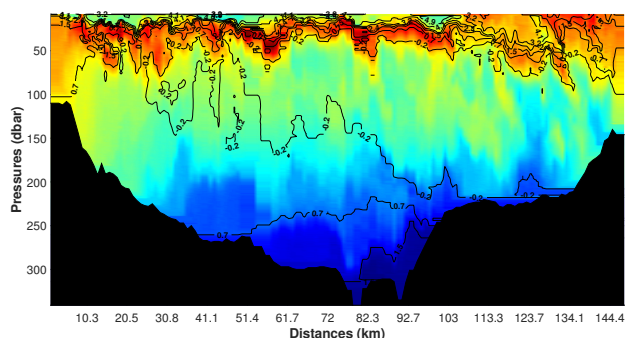
Figure 9. Cape Bathurst transect profiles during leg 4 of 2021 expedition. Isolines represent conservative temperature (isotherms, in $^{\circ}\text{C}$). The north-eastern side of the transect is located on the left.

3.2 MVP

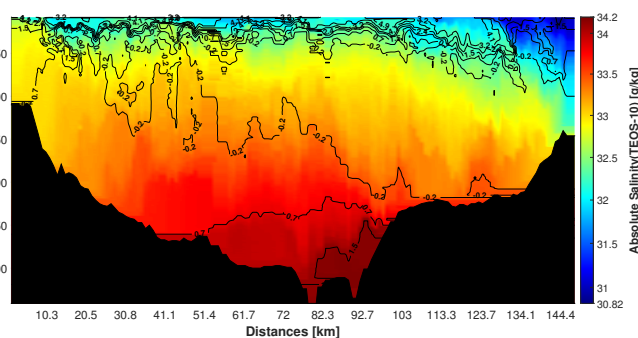
One MVP transect was conducted in Hudson Strait during leg 3 on August 14, 2021. A total of 197 casts (vertical dives) were carried out. The transects shown in Fig. 10b and Fig. 10c represent 148 casts (cast-1 to cast-148) arranged linearly from Baffin Island to the coast of Nunavik (left to right). The remaining set of casts (cast-149 to cast-197) were conducted across Diana Bay to reach Quaqtaq. Only the first 148 casts are presented in this paper. Quality Control assessment is applied at the final step of the data processing. Uncertainties of 0.01 PSU are observed when there is relatively low vertical variability, but high vertical gradient can increase these uncertainties. For the dissolved oxygen sensor on the MVP, the uncertainty is in the order of 1%. However, it may exceed the value of 1% when high vertical temperature and salinity gradient occur.



(a) MVP dive locations across Hudson Strait



(b) Dissolved Oxygen [mL/L]



(c) Absolute salinity [g/kg]

Figure 10. MVP section profile across Hudson Strait from leg 3 of the 2021 expedition.

Over the transect in Hudson Strait, the MVP dived approximately at each km, allowing high precision data recording. Mixing and turbulence are visible in Fig.10b, where the layer of maximum dissolved oxygen is overall well defined, but varies in depth over nearly 50 dbar. Lowest dissolved oxygen values are located in the center of the transect, below 200 dbar. Lower salinity values (below 32 g/kg) are located close to the coast of Nunavik, on the right-hand side of Fig.10c. This relatively fresh water mass is characteristic of the Hudson Bay outflow, the principal current linking the Hudson Bay System to the Labrador Sea, as described in previous studies (Ridenour et al., 2021; Straneo and Saucier, 2008). A layer of high salinity (> 34 g/kg), surrounded by the 1.5 ° conservative temperature isoline is observed at the bottom. Above this bottom layer lays a superposition of two layers of AS limited by CT values of 0.7 °C and -0.2 °C respectively. From the bottom to the surface, the variation of AS appears to be smoother compared to the variation of the DO. In general, the layer of high DO does not reflect the AS values anywhere near the surface (Fig.10c).

3.3 TSG

The underway thermosalinograph was operational during the five Legs of the CCGS *Amundsen* scientific expedition in 2021 but only sea surface absolute salinity (AS) derived from the practical salinity recorded during leg 2 from July 16 to August 12, 2021 is presented in 12. This subset was selected because of its high spacial variations. The minimum and maximum values of the absolute salinity ranges between 4.66-34.69 g/kg (average and median salinity of 31.04 g/kg and 31.59 g/kg respectively) in



accordance with previous observed values for Baffin Bay and Labrador Sea (Lavoie et al., 2013; Zweng and Münchow, 2006).
315 Lower values (fresher waters) are located in Scott Inlet and in the Clark and Gibbs Fjords (Nunavut), close to Qikiqtaaluk (Sillem) Island. Higher salinity is observed over the deeper regions of Labrador Sea and southern Baffin Bay. The close-up map in figure 12 shows the variation of the sea surface salinity at a location where fresh water masses meet the sea.

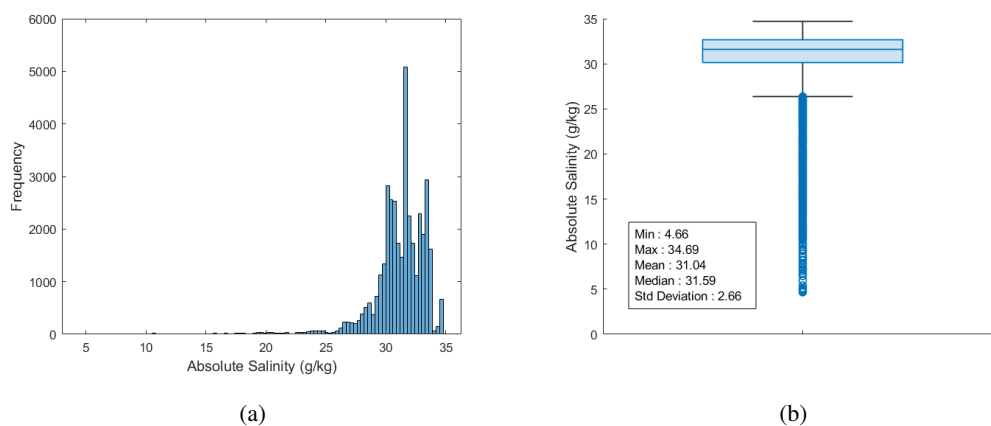


Figure 11. Histogram 11a and Boxplot 11b of the Absolute Salinity values from the TSG.

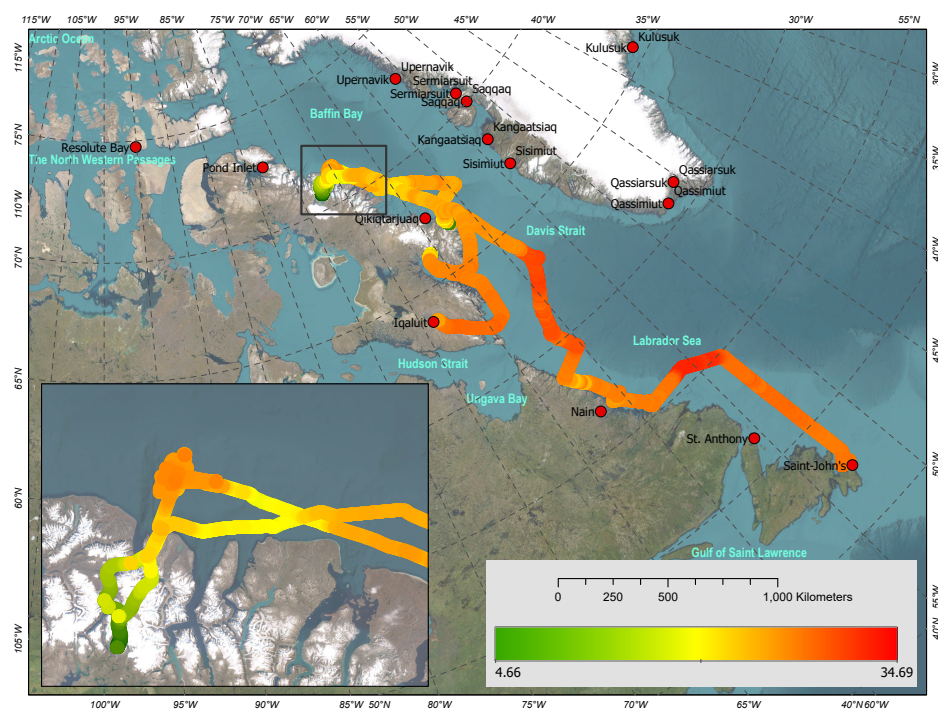


Figure 12. Absolute salinity (in g/kg) obtained from the underway TSG system during leg 2 of the 2021 expedition. (©ESRI 2023).

3.4 Atmospheric data

The Automated Voluntary Observing System (AVOS) recorded atmospheric and weather data continuously during the 2021
320 scientific expedition. Due to instrument malfunctions and errors identified during data processing, the percentage of data
reaching the quality standards described in Sect 2.3.2 varies between 44 % of acceptable values (relative humidity) and 97
% (atmospheric pressure), with an average of 67 % of acceptable values for all measured variables. Diurnal cycles and air
masses changes can be observed during an 8-days segment of leg 2, where the ship sailed in the Labrador Sea from offshore
Makkovik to Davis Strait (Fig. 13). A subset of four major variables (atmospheric pressure, surface photosynthetic active
325 radiation (SPAR), air temperature, and humidity) is presented and may be used to assess meteorological conditions during
other sampling operations and during transit. Such variables can be necessary to interpret other findings, as sea-surface physical
conditions and weather are closely related during sampling activities (Rohli and Li, 2021; Lin et al., 1996).

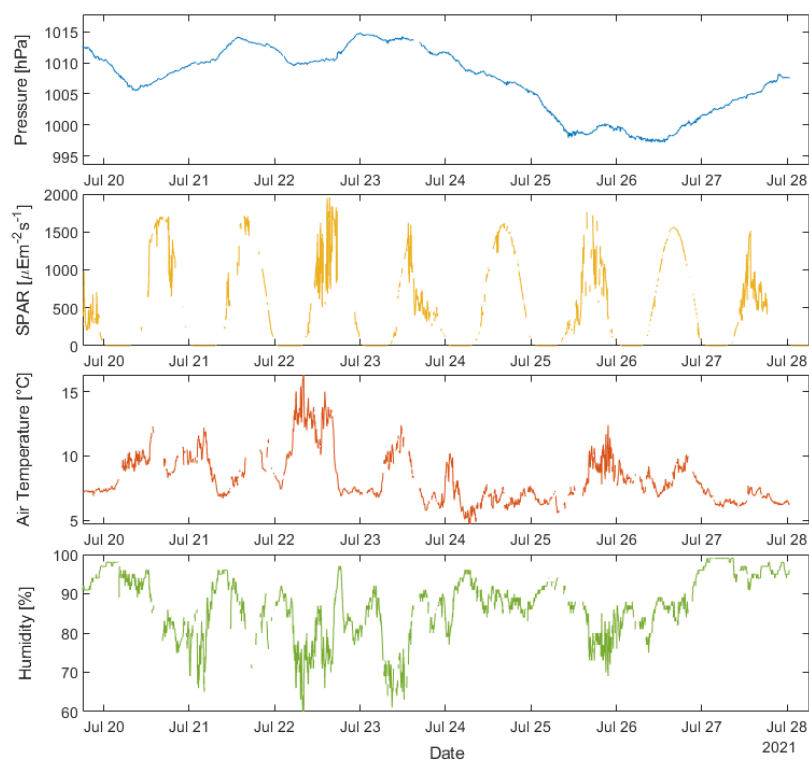


Figure 13. Atmospheric data from leg 2 of the 2021 expedition. Atmospheric pressure, surface photosynthetic active radiation (SPAR), air temperature and relative humidity were measured over 20-28 July 2021.



3.5 Seabed Data

Over the five legs of the 2021 expedition the scientific echo sounders onboard the CCGS *Amundsen* continuously collected data, accumulating approximately 38700 square kilometres of spatial coverage over a distance of nearly 17000 nautical miles (Table 5).

In addition to opportunistic data collection, dedicated seabed surveys provided primary and ancillary data sets to research projects. The following section presents two dedicated multibeam operations conducted during the 2021 Expedition. Data can be accessed on demand at amundsen.data@as.ulaval.ca.

Table 5. Scientific Echosounder spatial coverage, operational distance and operational time during the 2021 expedition

Leg	Spatial Coverage (km ²)	Distance (nm)	Duration (hours)
Leg 1	3495	1459	245
Leg 2	9539	3812	522
Leg 3	11135	3692	583
Leg 4	7193	3894	470
Leg 5	7303	4035	515

3.5.1 Makkovik

The hydrographic survey seen in Fig.14 was conducted offshore Makkovik (Nunatsiavut) during Leg 2. The survey zone is located 12 nautical miles from the coast of Makkovik where the seafloor ranges from 100-900 m depth in transition between coastal and deep areas, at the junction between the Aillik and Kaipokok domains of the Palaeoproterozoic Makkovik province (Peace et al., 2018). Several overlapping geological processes take place in this province and create a complex geological structure (Culshaw et al., 2000). The area was selected for this survey due to its topographic features and steep slopes, which may host conditions supporting coral habitats (Edinger et al., 2011; Wareham and Edinger, 2007).

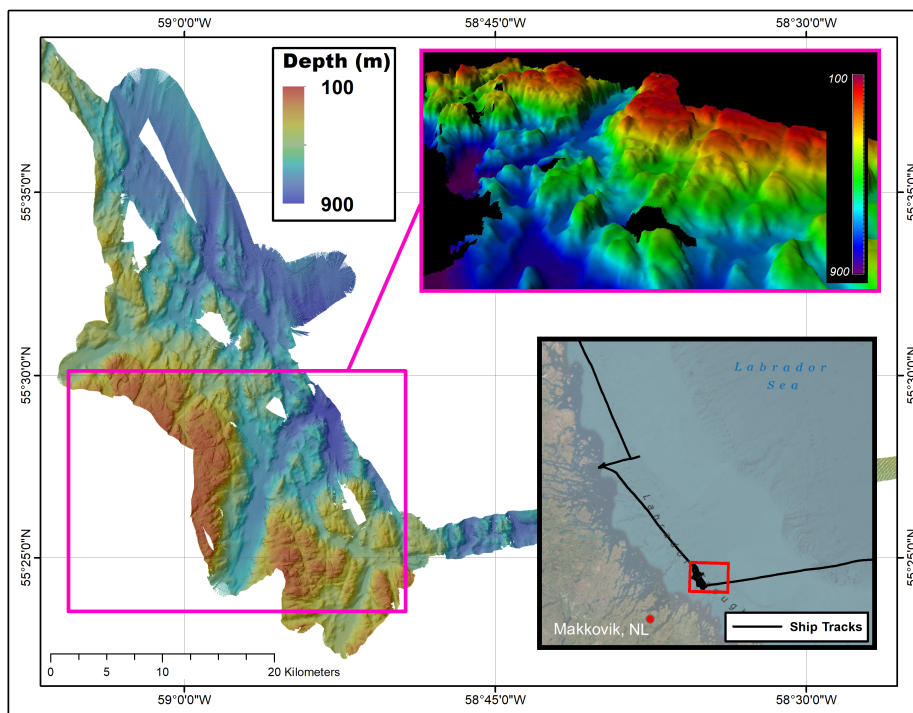


Figure 14. Hydrographic survey completed during leg 2 of the 2021 expedition. (©ESRI 2023)

3.5.2 Smith Bay

Little is known about the precise mechanisms linking the ocean-climate system and frontal positions of glaciers in the CAA (Cook et al., 2019). In order to characterise post-glacial history of Mittie Glacier and study the dynamics of glaciers in the
345 CAA (Amundsen Science, 2021b), bathymetric data (Fig.15) and in situ samples were collected in Smith Bay, Nunavut during Leg 3. In addition to the operation of CCGS *Amundsen* echosounders, a multibeam echosounder was installed and tested on the ship's barge along the terminus of Mittie Glacier.

Little to no seafloor data existed in Smith Bay prior to Leg 3 operations; the CCGS *Amundsen* collected the first publicly available high resolution seafloor topography data set in the area. Data depicted in Fig.15 will increase the efficiency and safety
350 of navigation for future operations in the area.

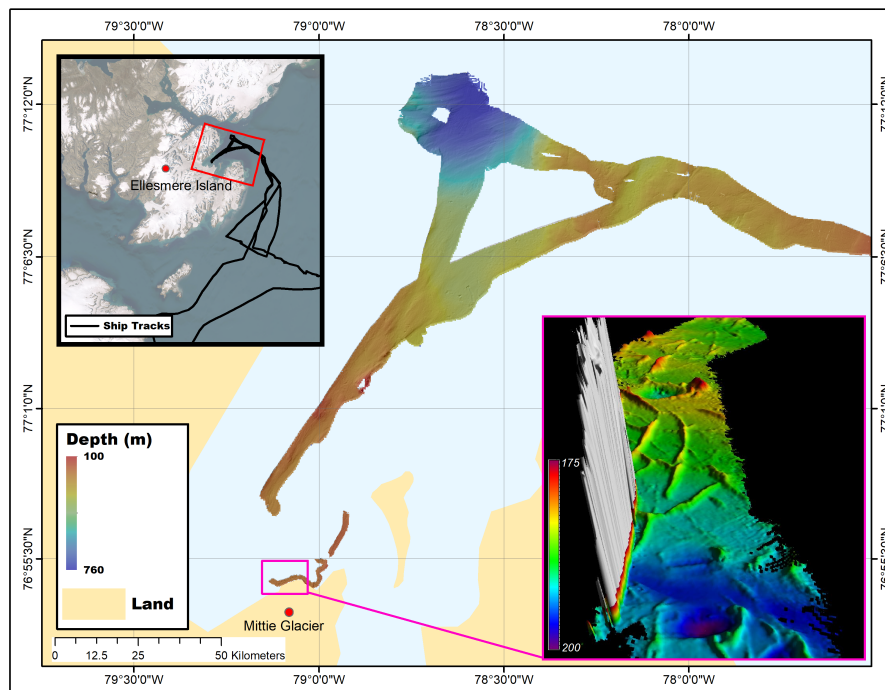


Figure 15. Hydrographic survey completed during Leg 3 of the 2021 expedition. (©ESRI 2023)



4 Conclusion

The vast amount of data collected by the central pool of equipment of the CCGS *Amundsen* during the 2021 scientific expedition in the Arctic can be used to study a vast array of research fields, from atmospheric environment to benthic ecosystems. Concurrent measurements above and under the sea surface provide invaluable tools to study the unique processes taking place in the Canadian and Greenlandic Arctic. The long-term monitoring of some of the regions of interest can allow studies of regional trends and variability. Similar research activities were also undertaken onboard other vessels in 2021 such as the USCGC Healy (McRaven, 2022) in Baffin Bay and can be used to validate or further refine findings. Only a few variable collected by the core data sets of scientific pool of equipment were presented in the paper and readers are invited to consult B1 for a comprehensive list of all data produced by the scientific community user of the CCGS *Amundsen* in 2021. Along with instruments presented in the paper, Amundsen Science is also responsible for managing a mono beam fish and zooplakton sonar (EK-80), 360 camera for ice concentration images, ROV video footage, moorings and navigation data.

Data sets collected during the scientific expedition of 2021 are archived and published in the Polar Data Catalogue for long term use. The metadata and data structures follow international standards to ensure findability and reusability of the data. Links to retrieve core data sets collected with the scientific pool of instruments onboard the CCGS *Amundsen* are available on the Amundsen Science web page, in the section Data Access at <https://amundsenscience.com/data/data-access/>. A complete list of instruments included onboard the CCGS *Amundsen* are available at <https://amundsenscience.com/canadian-research-icebreaker/scientific-equipment/>.

5 Data availability

Data availability All data are available on the Polar Data Catalogue with their DOI as follow:

- AVOS DOI: 10.5884/12518 (Science, 2021a)
- MVP DOI: 10.5884/12519 (Amundsen Science, 2021a)
- CTD Rosette DOI: 10.5884/12713 (Science, 2021b)
- TSG DOI: 10.5884/12715 (Science, 2021c)

6 Code availability

Code availability All the codes used for data processing and are available on Gitub as shown below:

- CTD Rosette:
- MVP: <https://git.valeria.science/amundsen/moving-vessel-profiler>
- TSG: <https://git.valeria.science/amundsen/thermosalinograph>

<https://doi.org/10.5194/essd-2023-204>
Preprint. Discussion started: 15 August 2023
© Author(s) 2023. CC BY 4.0 License.



– AVOS: <https://git.valeria.science/amundsen/avos>



380 Appendix A: Stations-ID (stations) geographical coordinates

Table A1. Station-ID located along Davis Strait transect.

Station ID	Time (UTC)	Latitude	Longitude
A1	2021-08-17T13:25:30	66.6054	-61.1941
A2	2021-08-17T19:22:58	66.6692	-60.4617
A3	2021-08-18T04:32:52	66.734	-59.6119
A4	2021-08-18T14:53:37	66.8026	-58.7708
A5	2021-08-19T01:02:50	66.8697	-57.9513
195	2021-08-19T10:35:01	66.8917	-56.9158
196	2021-08-19T17:05:43	66.9821	-56.0683
197	2021-08-19T21:53:33	67.0433	-55.0851
198	2021-08-20T01:38:55	67.0842	-54.201

Table A2. Stations-ID located along NOW transect.

Station-ID	Time (UTC)	Latitude	Longitude
116	2021-08-31T10:03:14	76.3802	-70.5147
115	2021-08-31T15:22:38	76.3314	-71.2046
114	2021-08-31T22:01:10	76.326	-71.7856
113	2021-08-31T23:14:28	76.3205	-72.2179
112	2021-09-01T01:02:36	76.3158	-72.7023
111	2021-09-01T02:51:48	76.3069	-73.2228
110	2021-09-01T05:35:18	76.2993	-73.6364
109	2021-09-01T07:30:44	76.291	-74.1154
108	2021-09-01T09:59:14	76.2641	-74.598
107	2021-09-01T16:29:57	76.2835	-75.0022
106	2021-09-01T19:20:46	76.3108	-75.3491
105	2021-09-01T20:56:45	76.3168	-75.7773
104	2021-09-02T00:09:18	76.3513	-76.2076
103	2021-09-02T00:59:08	76.3686	-76.548
102	2021-09-02T02:13:52	76.3745	-76.9784
101	2021-09-02T21:38:51	76.3848	-77.4143
100	2021-09-03T03:46:44	76.4105	-77.9564



Table A3. Stations-ID located along the Cape Bathurst Transect.

Station-ID	Time (UTC)	Latitude	Longitude
409	2021-09-18T19:06:34	71.8689	-125.8675
410	2021-09-18T23:44:42	71.6988	-126.4873
411	2021-09-19T01:20:22	71.6297	-126.7101
412	2021-09-19T02:30:56	71.5646	-126.9189
413	2021-09-19T04:16:47	71.4954	-127.1415
414	2021-09-19T06:28:18	71.4236	-127.3731
415	2021-09-19T11:06:50	71.3629	-127.5487
416	2021-09-19T12:15:51	71.2921	-127.7697
417	2021-09-19T13:41:45	71.2248	-127.97
418	2021-09-19T14:41:32	71.1633	-128.1672
419	2021-09-19T15:58:43	71.1067	-128.3449
420	2021-09-19T18:28:03	71.0517	-128.5139

Appendix B: Programs and data collected during the 2021 CCGS Amundsen Expedition

Table B 1: Programs and data collected during the 2021 CCGS Amundsen Expedition

Programs	Leg1	Leg2	Leg3	Leg4	Leg5	Data Collected Field of Study	Ship's Instrument	PI	Data status
Marine Spatial Planning program of Natural Resources Canada (NRCCan)	X	-	-	-	-	Sediment characterization	Piston Core, boxcores, bottom camera, Multibeam, sub bottom profilers	Vladimir (vladimir.kostylev@canada.ca)	Kostylev
Eastern Canada Seabirds at Sea (ECSAS) pelagic seabird surveys (EC)	X	X	X	-	-	Seabird abundance, diversity and distribution; opportunistic sightings of marine mammals and ocean pollution		Carina (carina.gjerdrum@ec.gc.ca)	Gjerdrum Already processed (i.e., archived in database)

Continued on next page



Table B1 – continued from previous page

Programs	Leg1	Leg2	Leg3	Leg4	Leg5	Data Collected Field of Study	Ship's Instrument	PI	Data status
Coral seep study project (DFO)	-	X	-	-	-	<p>(a) Benthos characterisation: Cold water corals, sponges and invertebrates abundance, distribution, and diversity.</p> <p>(b) Pelagic and Sympagic POM, Nutrient and $\delta^{15}\text{N}$-NO_3, Total inorganic carbon (TIC) and total alkalinity (TA), $p\text{CO}_2$ and CH_4.</p> <p>(c) $\delta^{13}\text{C}$AA and $\delta^{15}\text{N}$-AA signatures from sediment and zooplankton</p> <p>(d) eDNA - Benthic and Pelagic Community</p> <p>(e) Deepwater Faunal bioturbation and bioirrigation activity</p> <p>(f) Solenomonine analysis experiment in sediment</p> <p>(g) epifaunal colonization and settlement patterns</p> <p>(h) Sediment biogeochemistry and benthic pelagic nutrient coupling</p> <p>(i) Water and sediment microbial baseline communities for potential bioremediation of an oil spill (GENICE)</p> <p>(j) Mooring water and acoustic properties, organic pollutants</p>	<p>(a) ROV video footage, gravity core, drop camera, Box Core, Baited camera</p> <p>(b) CTD-Rosette, cage for ice sampling</p> <p>(c) boxcore, Hydrobios</p> <p>(d) CTD-Rosette</p> <p>(e) Box Core</p> <p>(f) Box Core</p> <p>(g) ROV-Box Core</p> <p>(h) BoxCore - ROV Push Core</p> <p>(i) ROV Niskin, CTD-Rosette, box core, ROV sediment sampling (sccop + push-Core)</p> <p>(j) Moorings with sediment trap, hydrophone, fish tag receiver and a semi-permeable membrane device (SPMD), current meter, CT sensor, AZFP</p>	<p>(a) David Cote (David.Cote@dfompo.gc.ca)</p> <p>(b) Owen Sherwood (Owen.Sherwood@dal.ca)</p> <p>(c) Owen Sherwood (Owen.Sherwood@dal.ca)</p> <p>(d) David Cote (David.Cote@dfompo.gc.ca)</p> <p>(e) Thomas Williams (T.J.Williams@stoton.ac.uk), Guillaume Blais (guillaume.blais.8@ulaval.ca)</p> <p>(f) Philippe Archambault (philippe.archambault@bio.ulaval.ca)</p> <p>(g) Annie Mercier (amercier@mun.ca)</p> <p>(h) Chris Algar (chris.algar@dal.ca)</p> <p>(i) Casey Hubert (chubert@ucalgary.ca)</p> <p>(j) David Cote (David.Cote@dfompo.gc.ca)</p>	<p>(a) in progress</p> <p>(b) in progress</p> <p>(c) in progress</p> <p>(d) in progress</p> <p>(e) in progress</p> <p>(f) in progress</p> <p>(g) in progress</p> <p>(h) in progress</p> <p>(i) in progress</p> <p>(j) in progress</p>

Continued on next page



Table B1 – continued from previous page

Programs	Leg1	Leg2	Leg3	Leg4	Leg5	Data Collected Field of Study	Ship's Instrument	PI	Data status
Atmospheric methane monitoring	-	X	-	-	-	Atmospheric and dissolved methane concentration	Met Tower- CTD-Rosette	Owen Sherwood (Owen.Sherwood@dai.ca)	In Progress - Judith Vogt PhD thesis (MUN), - defending summer 2022
ArcticNet-ArcticFish	-	X	X	X	-	distribution and ecology of key pelagic species in Arctic marine food webs- Fish and zooplankton	TuckerNet-MonsterNet--Hydrobios-IKMT-BeamTrawl-Continuous plankton recorder (PCR)-Baited remote underwater video (BRUV) camera - EK80 echosounder-WBAT	Maxime Geoffroy (maxime.geoffroy@mi.mun.ca), Jonathan Fisher (Jonathan.Fisher@mi.mun.ca), Dominique Robert (dominique_robert@uqar.ca)	Ichthyoplankton, fish, and macrozooplankton data processed and available upon request. Acoustics, mesozooplankton, and imagery data are being processed
ArcticNet Seafloor Mapping Project	-	X	X	X	-	Seafloor characterization, historical sea surface condition and biological condition. Marine geohazard. Diatoms/dinoflagellate distribution.	Piston Core, Gravity Core, box cores, Seabed mapping, sub bottom profilers, phytoplankton net, ROV, MSCL, Drop Camera, Mooring	Jean-Carlos Montero-Serrano (Jcancarlos_Monteroserrano@uqar.ca)	
ArcticNet-Biogeochemistry	-	X	X	X	-	Carbon Exchange Dynamics, Air-Surface Fluxes and Surface Climate : Dissolved O ₂ /CO ₂ , PH, Salinity, meteorology data	Underway seawater system (PCO ₂), Met tower, CTD-Rosette	Brent Else (belse@ucalgary.ca)	- Being processed, but fairly far along. Could provide example figure if needed. - In progress
ArcticNet-Biogeochemistry	-	-	X	-	-	Underway measurements of phytoplankton productivity and trace gases: Active Chlorophyll Fluorescence, O ₂ /N ₂ , CH ₄ /N ₂ , nutrients (NO ₃ -)	Underway seawater system	Philippe Tortell (ptortell@eoas.ubc.ca)	

Continued on next page



Table B1 – continued from previous page

Programs	Leg1	Leg2	Leg3	Leg4	Leg5	Data Collected Field of Study	Ship's Instrument	PI	Data status
Knowledge and Ecosystem Based Approach program in Baffin Bay (KEBABB) and Barrow Strait (KEBABS) (DFO)	-	-	X	-	-	<ul style="list-style-type: none"> Water column biochemistry: TIC/TIA, DOC/DN, Salinity, del18O, flow cytometry (FC), chlorophyll a, Phytoplankton taxonomy, Fatty acid (FA), POC/PN, FRRF Genomics Zooplankton Taxonomy and fatty Acids Sediment characterization Benthic Epifauna 	<ul style="list-style-type: none"> CTD-Rosette CTD-Rosette Hydrobios-TuckerNet-MonsterNet Box Core Agassiz-Beam trawl 	Christine Michel (christine.michel@dfo-mpo.gc.ca)	
ArcticNet-Go ICE	-	-	X	-	-	Glacier Velocity and Mass Balance, Iceberg Drift Tracking	Helicopter	Luke Copland (luke.copland@nottawa.ca), Wesley van Wychen (wesley.van.wychen@waterloo.ca)	Iceberg drift data has been processed and can be included in paper; glacier velocity data won't be downloaded until summer 2022
Sentinel North-Quaqtaq	-	-	X	X	-	Solenoneine analysis experiment in sediment	Box Core	Philippe Archambault (philippe.archambault@bio.ulaval.ca)	
Canadian Arctic Archipelago Rivers Program (CAA-RP) and ArcticNet Contaminants and Program	-	-	X	X	-	River sampling of dissolved organic carbon (DOC), dissolved major ions (Ca, Mg, Na, K, Cl, SO4) and minor ions (Sr, Ba), stable isotopes of water (oxygen-18 and deuterium), and dissolved nutrient concentrations (Nitrate, Phosphate, Silicate) Bedload sediment and glacial till sample	Helicopter	Jean-Carlos Montero-Serrano (Jcancarlos_Monterserrano@uqar.ca), Kristina Brown (Kristina.Brown@umanitoba.ca)	In progress, partial analyses completed (Nutrients, DOC, water isotopes), remaining samples archived for analyses in Spring 2023

Continued on next page



Table B1 – continued from previous page

Programs	Leg1	Leg2	Leg3	Leg4	Leg5	Data Collected Field of Study	Ship's Instrument	PI	Data status
ArcticNet-NTRAIN- GEOTRACES	-	-	X	X	-	dissolved micronutrient trace metals (Fe, Mn, Cu, Cd, Pb, Zn, Co, Ni) and Macronutrient	Go-flow (moon pool)	Jay Cullen (jcullen@uwic.ca)	In progress
ArcticNet-NTRAIN-Marine productivity	-	-	X	X	-	¹³ C/ ¹⁵ N incub., Nutrients, Nitrate isotopes, Ammonium, Stable isotopes, DOC/DON, POC/PN, BSi/POP, Fatty Acids, Total Lipids, Bio Markers, Taxonomy	CTD-Rosette	Jean-Éric Tremblay (jean-eric.tremblay@bio.ulaval.ca)	
Northern Contaminants Pro- gram (EC-Umanitoba))	-	-	X	X	-	Microplastic and Persistent Organic pollutant (POPs) in air, water, zooplankton and sediments	CTD-Rosette, surface water (bucket), Monsternet-Tucker Net	Liisa Jantunen (liisa.jantunen@ec.gc.ca)	being pro- cessed and already pro- cessed
Northern Contaminants Pro- gram (EC-Umanitoba))	-	-	-	X	-	Perfluorinated alkylated substances (PFAS), Organic contaminants (PAHs) and mercury within benthic and pelagic organisms.	Monsternet-Tucker Net - Beamtrawl	Gary Stern (gary.stern@umanitoba.ca)	Being pro- cessed
PECABEAU (EU-ARICE)	-	-	-	X	-	sediment and OM burial rates, concentration and composition of dissolved and particulate organic matter (DOM and POM), optical measurements (radiometry)	CTD rosette, Multicorer, Pis-ton core, Seabed mapping, MSCL,	Lisa Bröder (lisa.broeder@erdw.ethz.ch) Michael Fritz (michael.fritz@awi.de)	In progress

Continued on next page



Table B1 – continued from previous page

Programs	Leg1	Leg2	Leg3	Leg4	Leg5	Data Collected Field of Study	Ship's Instrument	PI	Data status
DARKEEDGE (Tukvik, Sentinel North)	-	-	-	-	X	(a) Wave, wind velocity, water temperature (b) Ice thickness (c) Near surface currents and turbulence, water temperature, relative humidity, air temperature, down-welling radiation (300-3000nm) (d) underice light properties, water column properties (e) CDOM (f) phytoplankton communities in new ice and water column (g) Condition of Calanus populations in terms of stage composition, vertical distribution, lipid content, activity patterns, and respiration rates (h) Marine productivity: Nutrients (NO ₃ , NO ₂ , PO ₄ , Si), NH ₄ , P _i , Kinetic (i) Water column properties- Biogeofloat	(a) Buoys (b) Ice Canoe (c) Flux-cat (Catamaran) (d) AUV with sensors for PAR, temperature, conductivity, nitrate concentration, irradiance, chlorophyll and CDOM fluorescence, and particulate backscattering - Small ROV - C-OPS (e) CTD-Rosette (f) CTD-Rosette, phytoplankton net, microscopy, genomics, cultures (g) Hydrobios-TuckerNet-MonsterNet-IKMT-WBAT-UVP (h) CTD-Rosette (i) ARGo float equipped with CTD, Radiometer: OCR wavelengths:380, 412, 490 nm, PAR, MPE (high sensitivity) PAR, fluorescence chl _a , fluorescence CDOM, Backscattering, Suna (nitrates), Optode (Oxygen) - Float equipped with UVP6	(a) Marcel Babin (marcel.babin@takvik.ulaval.ca) (b) Marcel Babin (marcel.babin@takvik.ulaval.ca) (c) Marcel Babin (marcel.babin@takvik.ulaval.ca) (d) Marcel Babin (marcel.babin@takvik.ulaval.ca) (e) Marcel Babin (marcel.babin@takvik.ulaval.ca) (f) Chris Bowler (cbowler@biologie.ens.fr) (g) Malin Duase (malin.duase@uit.no), Gérald Darnis (Gerald.Darnis@qc.ulaval.ca), Maxime Geoffroy (maxime.geoffroy@mi.mun.ca) (h) Jean-Éric Tremblay (jean-eric.tremblay@bio.ulaval.ca) (i) Marcel Babin (marcel.babin@takvik.ulaval.ca)	Data analysis in progress
RADCARBBS	-	-	-	X	-	Radiocarbon ($\Delta^{14}C$) and stable carbon ($\delta^{13}C$) isotopic measurements of dissolved inorganic carbon (DIC), dissolved organic carbon (DOC), and particulate organic carbon (POC)	CTD-Rosette	Brett Walker (brett.walker@uottawa.ca)	In progress, DOC/TN completed.

Continued on next page



Table B1 – continued from previous page

Programs	Leg1	Leg2	Leg3	Leg4	Leg5	Data Collected Field of Study	Ship's Instrument	PI	Data status
Community of Uluhaktok (Amundsen Science)	-	-	-	X	-	Underwater sound ecology, wave and current regime	benthic tripod with current meter, CT sensor, hydrophone	Alexandre (alexandre.forest@as.ulaval.ca)	Forest
ISECOLDISICLE	X	-	-	-	-	(a) Benthos characterisation: Cold water corals, sponges and invertebrates abundance, distribution, and diversity. (b) $\delta^{13}\text{C}_{\text{AA}}$ and $\delta^{15}\text{N}_{\text{AA}}$ signatures from sediment and zooplankton (c) eDNA - Benthic and Pelagic Community Characterization (d) epifaunal colonization and settlement patterns (e) Sediment biogeochemistry and benthic pelagic nutrient coupling (f) Mooring water and acoustic properties, organic pollutants (g) Distribution and ecology of key pelagic species in Arctic marine food webs- Fish and zooplankton (h) Contaminant load of fish in the Labrador Sea	(a) ROV video footage, gravity core, drop camera, Box Core, Baited camera (b) boxcore, Hydrobios (c) CTD-Rosette (d) ROV-Box Core-array retrieval (e) Box Core - ROV Push Core (f) Moorings with sediment trap, hydrophone, fish tag receiver and a semi-permeable membrane device (SPMD), current meter, CT sensor, AZFP (g) Hydrobios-IKMT- Beamtrawl- Baited remote underwater video (BRUV) camera- EK80 echosounder - WBAT (h) Hydrobios-IKMT	(a) David Cote (David.Cote@dfopmpo.gc.ca), Barbara.Neves@dfopmpo.gc.ca, Alexandre.Normandeau@nrcan.gc.ca (b) (c) David Cote (David.Cote@dfopmpo.gc.ca) (d) Annie Mercier (amercier@mum.ca) (e) Chris Algar (chris.algar@dal.ca) (f) David Cote (David.Cote@dfopmpo.gc.ca) (g) Maxime Geoffroy (maxime.geoffroy@mi.mun.ca), David.Cote@dfopmpo.gc.ca (h) Maxime Geoffroy (maxime.geoffroy@mi.mun.ca), David.Cote@dfopmpo.gc.ca	Data analysis in progress
CRSNG Discovery Archaic haul	X	-	-	-	-	Biology of shrimp in the Arctic (Shrimp's diet and eggs)	IKMT	Philippe Archambault(philippe.archambault@bio.ulaval.ca), Maxime Geoffroy (maxime.geoffroy@mi.mun.ca), Guillaume Blais (guillaume.blais.8@ulaval.ca)	Data analysis in progress



Appendix C: Additional figures

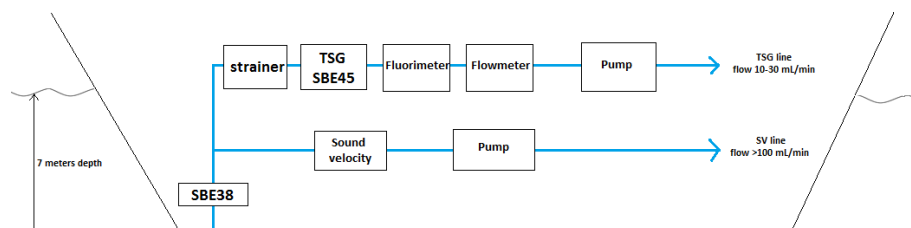


Figure C1. Thermosalinograph Schematic
Schematic of the TSG

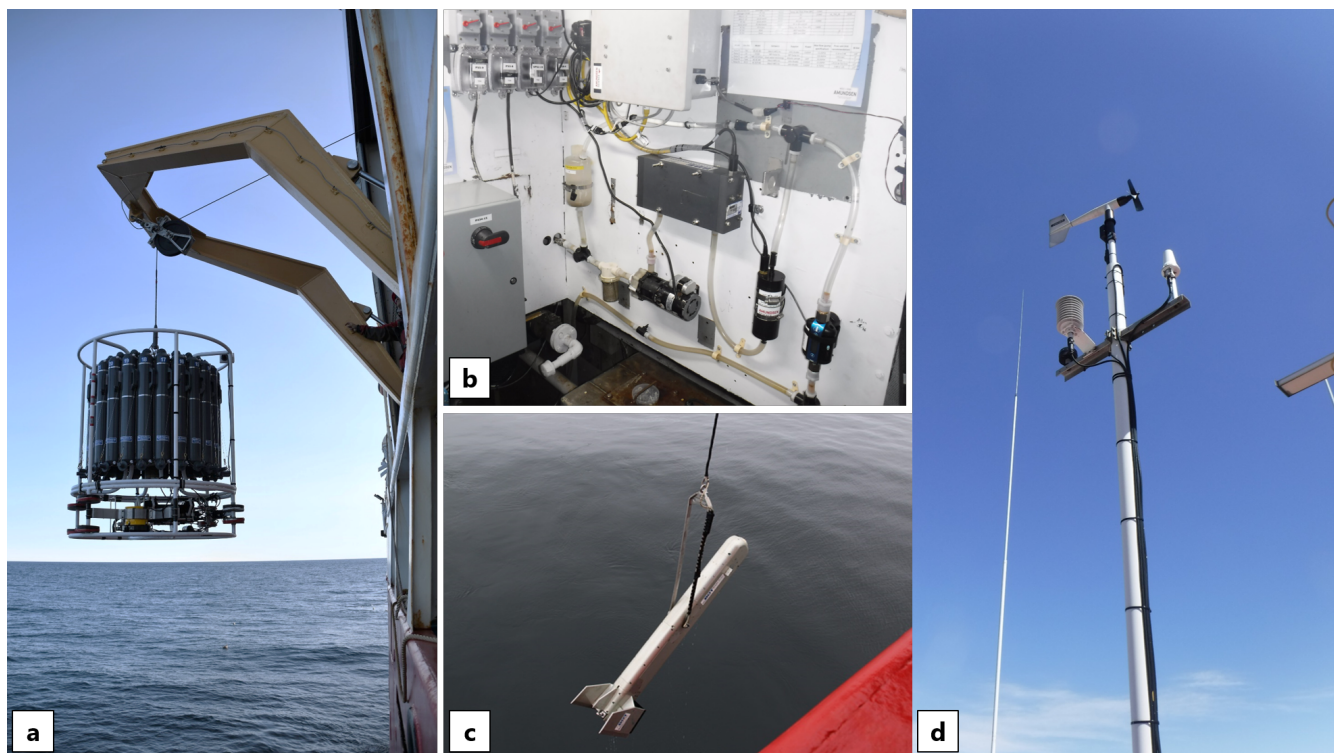


Figure C2. Photo of (a) the CTD Rosette being deployed with the A-Frame, (b) the TSG in the engine room, (c) the MVP fish being deployed and (d) the AVOS system.

Author contributions. These authors contributed equally to this work.



385 *Acknowledgements.* We thank the commanding officers and crews of the CCGS *Amundsen* for providing support during the entire 2021 expedition. This sampling could not have been undertaken without the interest and contribution of the scientific community and user programs. We thank Philippe Massicotte (Université Laval) for providing suggestions. This work was supported by the Major Scientific Infrastructure fund of the Canada Foundation for Innovation.



References

- Adams, J. K., Dean, B. Y., Athey, S. N., Jantunen, L. M., Bernstein, S., Stern, G., Diamond, M. L., and Finkelstein, S. A.: Anthropogenic particles (including microfibers and microplastics) in marine sediments of the Canadian Arctic, *Science of The Total Environment*, 784, 147–155, <https://doi.org/https://doi.org/10.1016/j.scitotenv.2021.147155>, 2021.
- Amundsen Science: Moving Vessel Profiling (MVP) data collected by the CCGS Amundsen in the Canadian Arctic., <https://doi.org/10.5884/12519>, 2021a.
- Amundsen Science: 2021 Expedition Report, Tech. rep., Amundsen Science, Université Laval, Québec, <https://amundsenscience.com/wp-content/uploads/2022/03/2021-Amundsen-Expedition-Report-2022-03-16-compressed.pdf>, 2021b.
- Arctic Council's Working Group on the Protection of the Arctic Marine Environment (PAME): Arctic Shipping Status Report 1, Tech. rep., <https://pame.is/document-library/pame-reports-new/pame-ministerial-deliverables/2021-12th-arctic-council-ministerial-meeting-reykjavik-iceland/793-assr-1-the-increase-in-arctic-shipping-2013-2019/file>, 2020.
- Arctic Monitoring and Assessment Programme (AMAP): 2018 AMAP Assessment - Arctic ocean acidification, Tech. rep., Arctic Monitoring and Assessment Programme, <https://www.amap.no/documents/doc/amap-assessment-2018-arctic-ocean-acidification/1659>, 2018.
- Armitage, T. W. K., Manucharyan, G. E., Petty, A. A., Kwok, R., and Thompson, A. F.: Enhanced eddy activity in the Beaufort Gyre in response to sea ice loss, *Nature Communications*, 11, <https://doi.org/10.1038/s41467-020-14449-z>, 2020.
- Arrigo, K. R. and van Dijken, G. L.: Annual cycles of sea ice and phytoplankton in Cape Bathurst polynya, southeastern Beaufort Sea, Canadian Arctic, *Geophysical Research Letters*, 31, <https://doi.org/https://doi.org/10.1029/2003GL018978>, 2004.
- Azetsu-Scott, K., Jones, E. P., Yashayaev, I., and Gershay, R. M.: Time series study of CFC concentrations in the Labrador Sea during deep and shallow convection regimes (1991–2000), *Journal of Geophysical Research: Oceans*, 108, <https://doi.org/https://doi.org/10.1029/2002JC001317>, 2003.
- Bamber, J. L., Tedstone, A. J., King, M. D., Howat, I. M., Enderlin, E. M., van den Broeke, M. R., and Noel, B.: Land Ice Freshwater Budget of the Arctic and North Atlantic Oceans: 1. Data, Methods, and Results, *Journal of Geophysical Research: Oceans*, 123, 1827–1837, <https://doi.org/https://doi.org/10.1002/2017JC013605>, 2018.
- Biospherical Instruments Inc.: http://www.biospherical.com/images/pdf/qcp2300_apr2014.pdf, 2014.
- Bâcle, J., Carmack, E. C., and Ingram, R.: Water column structure and circulation under the North Water during spring transition: April/July 1998, *Deep Sea Research Part II: Topical Studies in Oceanography*, 49, 4907–4925, [https://doi.org/https://doi.org/10.1016/S0967-0645\(02\)00170-4](https://doi.org/https://doi.org/10.1016/S0967-0645(02)00170-4), the International North Water Polynya Study, 2002.
- Carmack, E. C. and Macdonald, R. W., eds.: *Oceanography of the Canadian Shelf of the Beaufort Sea: A Setting for Marine Life*, vol. Vol. 55 No. 5 (2002): Supplement: 1–93 of The Beaufort Sea Conference 2000, Arctic Institute of North America, <https://doi.org/https://doi.org/10.14430/arctic733>, 2002.
- Carson, M. A., Jasper, J. N., and Conly, F. M.: Magnitude and Sources of Sediment Input to the Mackenzie Delta, Northwest Territories, 1974–94, *Arctic*, 51, 116–124, <http://www.jstor.org/stable/40488391>, 1998.
- Clarke, R. A. and Coote, A. R.: The Formation of Labrador Sea Water. Part III: The Evolution of Oxygen and Nutrient Concentration, *Journal of Physical Oceanography*, 18, 469–480, [https://doi.org/10.1175/1520-0485\(1988\)018<0469:TFOLSW>2.0.CO;2](https://doi.org/10.1175/1520-0485(1988)018<0469:TFOLSW>2.0.CO;2), 1988.
- Comiso, J. C.: A rapidly declining perennial sea ice cover in the Arctic, *Geophysical Research Letters*, 29, 17–1–17–4, <https://doi.org/https://doi.org/10.1029/2002GL015650>, 2002.



- 425 Commission, I. O. et al.: *GTSP Real-Time Quality Control Manual. Revised edition 2010.*, https://unesdoc.unesco.org/notice?id=p::usmarcdef_0000190563, 2010.
- Cook, A. J., Copland, L., Noël, B. P. Y., Stokes, C. R., Bentley, M. J., Sharp, M. J., Bingham, R. G., and Van Den Broeke, M. R.: Atmospheric forcing of rapid marine-terminating glacier retreat in the Canadian Arctic Archipelago, *Science Advances*, 5, <https://doi.org/10.1126/sciadv.aau8507>, 2019.
- 430 Copland, L., Sharp, M. J., and Dowdeswell, J. A.: The distribution and flow characteristics of surge-type glaciers in the Canadian High Arctic, *Annals of Glaciology*, 36, 73–81, <https://doi.org/10.3189/172756403781816301>, 2003.
- Culshaw, N., Ketchum, J., and Barr, S.: Structural evolution of the Makkovik Province, Labrador, Canada: Tectonic processes during 200 Myr at a Paleoproterozoic active margin, *Tectonics*, 19, 961–977, <https://doi.org/https://doi.org/10.1029/1999TC001156>, 2000.
- Curry, B., Lee, C. M., and Petrie, B.: Volume, Freshwater, and Heat Fluxes through Davis Strait, 2004–05, *Journal of Physical Oceanography*, 41, 429–436, <https://doi.org/10.1175/2010JPO4536.1>, 2011.
- 435 Dawson, J., Pizzolato, L., Howell, S. E. L., Copland, L., and Johnston, M. E.: Temporal and Spatial Patterns of Ship Traffic in the Canadian Arctic from 1990 to 2015, Vol. 71, <https://doi.org/https://doi.org/10.14430/arctic4698>, 2018.
- DeGrandpre, M. D., Körtzinger, A., Send, U., Wallace, D. W. R., and Bellerby, R. G. J.: Uptake and sequestration of atmospheric CO₂ in the Labrador Sea deep convection region, *Geophysical Research Letters*, 33, <https://doi.org/https://doi.org/10.1029/2006GL026881>, 2006.
- Dezutter, T., Lalande, C., Darnis, G., and Fortier, L.: Seasonal and interannual variability of the Queen Maud Gulf ecosystem derived from sediment trap measurements, *Limnology and Oceanography*, 66, S411–S426, <https://doi.org/https://doi.org/10.1002/lno.11628>, 2021.
- 440 Dickson, D. L. and Gilchrist, H. G., eds.: Status of Marine Birds of the Southeastern Beaufort Sea, vol. Vol. 55 No. 5 (2002): Supplement: 1–93 of The Beaufort Sea Conference 2000, Arctic Institute of North America, <https://doi.org/https://doi.org/10.14430/arctic734>, 2002.
- Dunmall, K., McNicholl, D., and Reist, J.: Community-based Monitoring Demonstrates Increasing Occurrences and Abundances of Pacific Salmon in the Canadian Arctic from 2000 to 2017, <https://doi.org/10.23849/npafctr11/87.90>, 2018.
- 445 Edinger, E. N., Sherwood, O. A., Piper, D. J., Wareham, V. E., Baker, K. D., Gilkinson, K. D., and Scott, D. B.: Geological features supporting deep-sea coral habitat in Atlantic Canada, *Continental Shelf Research*, 31, S69–S84, <https://doi.org/https://doi.org/10.1016/j.csr.2010.07.004>, geological and Biological Mapping and Characterisation of Benthic Marine Environments, 2011.
- Environment and Canada, C. C.: Environment and Climate Change Canada (2021) Canadian Environmental Sustainability Indicators: Sea ice in Canada, <https://www.canada.ca/en/environment-climate-change/services/environmental-indicators/seaice.html>, 2021a.
- 450 Environment and Canada, N. R.: Environment and Natural Resources Canada (2021) Climate data viewer, <http://web.archive.org/web/20080207010024/https://climate-viewer.canada.ca/climate-maps.html>, 2021b.
- Falk-Petersen, S., Pavlov, V., Timofeev, S., and Sargent, J. R.: Climate variability and possible effects on arctic food chains: The role of *Calanus*, pp. 147–166, Springer Berlin Heidelberg, Berlin, Heidelberg, https://doi.org/10.1007/978-3-540-48514-8_9, 2007.
- 455 Galley, R. J., Babb, D., Ogi, M., Else, B. G. T., Geilfus, N.-X., Crabeck, O., Barber, D. G., and Rysgaard, S.: Replacement of multiyear sea ice and changes in the open water season duration in the Beaufort Sea since 2004, *Journal of Geophysical Research: Oceans*, 121, 1806–1823, <https://doi.org/https://doi.org/10.1002/2015JC011583>, 2016.
- Gearheard, S., Pocernich, M., Stewart, R., Sanguya, J., and Huntington, H. P.: Linking Inuit knowledge and meteorological station observations to understand changing wind patterns at Clyde River, Nunavut, *Climatic Change*, 100, 294, <https://doi.org/10.1007/s10584-009-9587-1>, 2010.
- 460 Guillot, P., Ratsimbazafy, T., and Thibaud, D.: <https://git.valeria.science/amundsen/2021-data-paper-codes-repository>, 2022.



- Gulev, S., Thorne, P., Ahn, J., Dentener, F., Domingues, C., Gerland, S., Gong, D., Kaufman, D., Nnamchi, H., Quaaas, J., Rivera, J., Sathyendranath, S., Smith, S., Trewin, B., von Schuckmann, K., and Vose, R.: *Changing State of the Climate System*, p. 287–422, Cambridge University Press, Cambridge, United Kingdom and New York, NY, USA, <https://doi.org/10.1017/9781009157896.004>, 2021.
- 465 Halliday, W. D., Dawson, J., Yurkowski, D. J., Doniol-Valcroze, T., Ferguson, S. H., Gjerdrum, C., Hussey, N. E., Kochanowicz, Z., Mallory, M. L., Marcoux, M., Watt, C. A., and Wong, S. N.: *Vessel risks to marine wildlife in the Tallurutiup Imanga National Marine Conservation Area and the eastern entrance to the Northwest Passage*, *Environmental Science & Policy*, 127, 181–195, <https://doi.org/https://doi.org/10.1016/j.envsci.2021.10.026>, 2022.
- Harwood, L. A. and Stirling, I.: *Distribution of ringed seals in the southeastern Beaufort Sea during late summer*, *Canadian Journal of*
470 *Zoology*, 70, 891–900, <https://doi.org/10.1139/z92-127>, 1992.
- Hauser, D. D. W., Laidre, K. L., Stafford, K. M., Stern, H. L., Suydam, R. S., and Richard, P. R.: *Decadal shifts in autumn migration timing by Pacific Arctic beluga whales are related to delayed annual sea ice formation*, *Global Change Biology*, 23, 2206–2217, <https://doi.org/https://doi.org/10.1111/gcb.13564>, 2017.
- Helle, I., Mäkinen, J., Nevalainen, M., Afenyo, M., and Vanhatalo, J.: *Impacts of oil spills on Arctic marine ecosystems: A quantitative and*
475 *probabilistic risk assessment perspective*, *Environ. Sci. Technol.*, 54, 2112–2121, 2020.
- Higdon, J. W. and Ferguson, S. H.: *Loss of Arctic sea ice causing punctuated change in sightings of killer whales (*Orcinus orca*) over the past century*, *Ecological Applications*, 19, 1365–1375, <https://doi.org/https://doi.org/10.1890/07-1941.1>, 2009.
- Hoover, C., Walkusz, W., MacPhee, S., Niemi, A., Majewski, A., and Loseto, L.: *Canadian Beaufort Sea Shelf Food Web Structure and Changes from 1970–2012*, *Tech. Rep. Canadian Data Report of Fisheries and Aquatic Sciences 1313, Central and Arctic Region*, Fisheries and
480 *Oceans Canada*, 501 University Crescent, Winnipeg, MB R3T 2N6, 2021.
- Howell, S. E. L. and Brady, M.: *The Dynamic Response of Sea Ice to Warming in the Canadian Arctic Archipelago*, *Geophysical Research Letters*, 46, 13 119–13 125, <https://doi.org/https://doi.org/10.1029/2019GL085116>, 2019.
- Hutchings, J. K. and Rigor, I. G.: *Role of ice dynamics in anomalous ice conditions in the Beaufort Sea during 2006 and 2007*, *Journal of Geophysical Research: Oceans*, 117, <https://doi.org/https://doi.org/10.1029/2011JC007182>, 2012.
- 485 Jakobsson, M., Cherkis, N., Woodward, J., Macnab, R., and Coakley, B.: *New grid of Arctic bathymetry aids scientists and mapmakers*, *Eos, Transactions American Geophysical Union*, 81, 89–96, <https://doi.org/https://doi.org/10.1029/00EO00059>, 2000.
- Jakobsson, M., Macnab, R., Mayer, L., Anderson, R., Edwards, M., Hatzky, J., Schenke, H. W., and Johnson, P.: *An improved bathymetric portrayal of the Arctic Ocean: Implications for ocean modeling and geological, geophysical and oceanographic analyses*, *Geophysical Research Letters*, 35, <https://doi.org/https://doi.org/10.1029/2008GL033520>, 2008.
- 490 Jakobsson, M., Mayer, L., Coakley, B., Dowdeswell, J. A., Forbes, S., Fridman, B., Hodnesdal, H., Noormets, R., Pedersen, R., Rebesco, M., Schenke, H. W., Zarayskaya, Y., Accettella, D., Armstrong, A., Anderson, R. M., Bienhoff, P., Camerlenghi, A., Church, I., Edwards, M., Gardner, J. V., Hall, J. K., Hell, B., Hestvik, O., Kristoffersen, Y., Marcussen, C., Mohammad, R., Mosher, D., Nghiem, S. V., Pedrosa, M. T., Travaglini, P. G., and Weatherall, P.: *The International Bathymetric Chart of the Arctic Ocean (IBCAO) Version 3.0*, *Geophysical Research Letters*, 39, <https://doi.org/https://doi.org/10.1029/2012GL052219>, 2012.
- 495 Johnston, M., Dawson, J., De Souza, E., and Stewart, E. J.: *Management challenges for the fastest growing marine shipping sector in Arctic Canada: pleasure crafts*, *Polar Record*, 53, 67–78, <https://doi.org/10.1017/S0032247416000565>, 2017.
- Kieke, D. and Yashayaev, I.: *Studies of Labrador Sea Water formation and variability in the subpolar North Atlantic in the light of international partnership and collaboration*, *Progress in Oceanography*, 132, 220–232, <https://doi.org/https://doi.org/10.1016/j.pocean.2014.12.010>, *oceanography of the Arctic and North Atlantic Basins*, 2015.



- 500 Kieke, D., Klein, B., Stramma, L., Rhein, M., and Koltermann, K. P.: Variability and propagation of Labrador Sea Water in the southern subpolar North Atlantic, *Deep Sea Research Part I: Oceanographic Research Papers*, 56, 1656–1674, <https://doi.org/https://doi.org/10.1016/j.dsr.2009.05.010>, 2009.
- Kwok, R.: Variability of Nares Strait ice flux, *Geophysical Research Letters*, 32, 2005.
- Kwok, R., Cunningham, G. F., Wensnahan, M., Rigor, I., Zwally, H. J., and Yi, D.: Thinning and volume loss of the Arctic Ocean sea ice cover: 2003–2008, *Journal of Geophysical Research: Oceans*, 114, <https://doi.org/https://doi.org/10.1029/2009JC005312>, 2009.
- 505 Kwok, R., Toudal Pedersen, L., Gudmandsen, P., and Pang, S. S.: Large sea ice outflow into the Nares Strait in 2007, *Geophysical Research Letters*, 37, <https://doi.org/https://doi.org/10.1029/2009GL041872>, 2010.
- Körtzinger, A., Send, U., Wallace, D. W. R., Karstensen, J., and DeGrandpre, M.: Seasonal cycle of O₂ and pCO₂ in the central Labrador Sea: Atmospheric, biological, and physical implications, *Global Biogeochemical Cycles*, 22, <https://doi.org/https://doi.org/10.1029/2007GB003029>, 2008.
- 510 Lansard, B., Mucci, A., Miller, L. A., Macdonald, R. W., and Gratton, Y.: Seasonal variability of water mass distribution in the southeastern Beaufort Sea determined by total alkalinity and $\delta^{18}\text{O}$, *Journal of Geophysical Research: Oceans*, 117, <https://doi.org/https://doi.org/10.1029/2011JC007299>, 2012.
- Lavoie, D., Lambert, N., and van der Baaren, A.: Projections of future physical and biogeochemical conditions in Hudson and Baffin bays from CMIP5 Global Climate Models, *Can. Tech. Rep. Hydrogr. Ocean Sci.*, pp. xiii + 129 pp, 2013.
- 515 Lehmann, N., Kienast, M., Granger, J., Bourbonnais, A., Altabet, M. A., and Tremblay, J.-E.: Remote Western Arctic Nutrients Fuel Remineralization in Deep Baffin Bay, *Global Biogeochemical Cycles*, 33, 649–667, <https://doi.org/https://doi.org/10.1029/2018GB006134>, 2019.
- Lin, C. A., Greatbatch, R. J., and Zhang, S.: Large Scale Atmosphere-Ocean Interaction and Climate, in: *Climate Sensitivity to Radiative Perturbations*, edited by Treut, H. L., pp. 291–303, Springer Berlin Heidelberg, Berlin, Heidelberg, 1996.
- 520 Lindsay, R. and Schweiger, A.: Arctic sea ice thickness loss determined using subsurface, aircraft, and satellite observations, *The Cryosphere*, 9, 269–283, <https://doi.org/10.5194/tc-9-269-2015>, 2015.
- Lobb, J., Carmack, E. C., Ingram, R. G., and Weaver, A. J.: Structure and mixing across an Arctic/Atlantic front in northern Baffin Bay, *Geophysical Research Letters*, 30, <https://doi.org/https://doi.org/10.1029/2003GL017755>, 2003.
- 525 Marko, J. R., Fissel, D. B., de Saavedra Álvarez, M. M., Ross, E., and Kerr, R.: Iceberg severity off the east coast of North America in relation to upstream sea ice variability: An update, in: *2014 Oceans - St. John's*, pp. 1–6, <https://doi.org/10.1109/OCEANS.2014.7003128>, 2014.
- Massicotte, P., Amiraux, R., Amyot, M.-P., Archambault, P., Ardyna, M., Arnaud, L., Artigue, L., Aubry, C., Ayotte, P., Bécu, G., Bélanger, S., Benner, R., Bittig, H. C., Bricaud, A., Brossier, E., Bruyant, F., Chauvaud, L., Christiansen-Stowe, D., Claustre, H., Cornet-Barthaux, V., Coupel, P., Cox, C., Delaforge, A., Dezutter, T., Dimier, C., Domine, F., Dufour, F., Dufresne, C., Dumont, D., Ehn, J., Else, B., Ferland, J., Forget, M.-H., Fortier, L., Galí, M., Galindo, V., Gallinari, M., Garcia, N., Gérikas Ribeiro, C., Gourdal, M., Gourvil, P., Goyens, C., Grondin, P.-L., Guillot, P., Guilmette, C., Houssais, M.-N., Joux, F., Lacour, L., Lacour, T., Lafond, A., Lagunas, J., Lalande, C., Laliberté, J., Lambert-Girard, S., Larivière, J., Lavaud, J., LeBaron, A., Leblanc, K., Le Gall, F., Legras, J., Lemire, M., Levasseur, M., Leymarie, E., Leynaert, A., Lopes dos Santos, A., Lourenço, A., Mah, D., Marec, C., Marie, D., Martin, N., Marty, C., Marty, S., Massé, G., Matsuoka, A., Matthes, L., Moriceau, B., Muller, P.-E., Mundy, C.-J., Neukermans, G., Oziel, L., Panagiotopoulos, C., Pangrazi, J.-J., Picard, G., Picheral, M., Pinczon du Sel, F., Pogorzelec, N., Probert, I., Quéguiner, B., Raimbault, P., Ras, J., Rehm, E., Reimer, E., Rontani, J.-F., Rysgaard, S., Saint-Béat, B., Sampei, M., Sansoulet, J., Schmechtig, C., Schmidt, S., Sempéré, R., Sévigny, C., Shen, Y., Tragin, M., Tremblay, J.-E., Vaultot, D., Verin, G., Vivier, F., Vladioiu, A., Whitehead, J., and Babin, M.: Green Edge ice camp campaigns:
- 535



- understanding the processes controlling the under-ice Arctic phytoplankton spring bloom, *Earth System Science Data*, 12, 151–176, <https://doi.org/10.5194/essd-12-151-2020>, 2020.
- 540 Massicotte, P., Amon, R. M. W., Antoine, D., Archambault, P., Balzano, S., Bélanger, S., Benner, R., Boeuf, D., Bricaud, A., Bruyant, F., Chaillou, G., Chami, M., Charrière, B., Chen, J., Claustre, H., Coupel, P., Delsaut, N., Doxaran, D., Ehn, J., Fichot, C., Forget, M.-H., Fu, P., Gagnon, J., Garcia, N., Gasser, B., Ghiglione, J.-F., Gorsky, G., Gosselin, M., Gourvil, P., Gratton, Y., Guillot, P., Heipieper, H. J., Heussner, S., Hooker, S. B., Huot, Y., Jeanthon, C., Jeffrey, W., Joux, F., Kawamura, K., Lansard, B., Leymarie, E., Link, H., Lovejoy, C., Marec, C., Marie, D., Martin, J., Martín, J., Massé, G., Matsuoka, A., McKague, V., Mignot, A., Miller, W. L., Miquel, J.-C., Mucci, A.,
- 545 Ono, K., Ortega-Retuerta, E., Panagiotopoulos, C., Papakyriakou, T., Picheral, M., Prieur, L., Raimbault, P., Ras, J., Reynolds, R. A., Rochon, A., Rontani, J.-F., Schmechtig, C., Schmidt, S., Sempéré, R., Shen, Y., Song, G., Stramski, D., Tachibana, E., Thirouard, A., Tolosa, I., Tremblay, J.-E., Vaïtilingom, M., Vaultot, D., Vaultier, F., Volkman, J. K., Xie, H., Zheng, G., and Babin, M.: *The MALINA oceanographic expedition: how do changes in ice cover, permafrost and UV radiation impact biodiversity and biogeochemical fluxes in the Arctic Ocean?*, *Earth System Science Data*, 13, 1561–1592, <https://doi.org/10.5194/essd-13-1561-2021>, 2021.
- 550 McCartney, M.: *Recirculating components to the deep boundary current of the northern North Atlantic*, *Progress in Oceanography*, 29, 283–383, [https://doi.org/https://doi.org/10.1016/0079-6611\(92\)90006-L](https://doi.org/https://doi.org/10.1016/0079-6611(92)90006-L), 1992.
- McDougall, T., Feistel, R., Millero, F., Jackett, D., Wright, D., King, B., Marion, G., Chen, C., Spitzer, P., and Seitz, S.: *The international thermodynamic equation of seawater 2010 (TEOS-10): Calculation and use of thermodynamic properties*, *Global ship-based repeat hydrography manual*, IOCCP report no, 14, 2009.
- 555 McDougall, T. J. and Barker, P. M.: *Getting started with TEOS-10 and the Gibbs Seawater (GSW) oceanographic toolbox*, *Scor/Iapso WG*, 127, 1–28, 2011.
- McGeehan, T. and Maslowski, W.: *Evaluation and control mechanisms of volume and freshwater export through the Canadian Arctic Archipelago in a high-resolution pan-Arctic ice-ocean model*, *Journal of Geophysical Research: Oceans*, 117, <https://doi.org/https://doi.org/10.1029/2011JC007261>, 2012.
- 560 McRaven, L.: *Shipboard hydrographic measurements from the Fate of freshwater and heat from the West Greenland Current project (2021)*, *Arctic Data Center*, <https://doi.org/10.18739/A2DB7VR5M>, 2022.
- Meier, W. N., Hovelsrud, G. K., van Oort, B. E., Key, J. R., Kovacs, K. M., Michel, C., Haas, C., Granskog, M. A., Gerland, S., Perovich, D. K., Makshtas, A., and Reist, J. D.: *Arctic sea ice in transformation: A review of recent observed changes and impacts on biology and human activity*, *Reviews of Geophysics*, 52, 185–217, <https://doi.org/https://doi.org/10.1002/2013RG000431>, 2014.
- 565 Melling, H., Gratton, Y., and Ingram, G.: *Ocean circulation within the North Water polynya of Baffin Bay*, *Atmosphere-Ocean*, 39, 301–325, <https://doi.org/10.1080/07055900.2001.9649683>, 2001.
- Michel, C., Ingram, R., and Harris, L.: *Variability in oceanographic and ecological processes in the Canadian Arctic Archipelago*, *Progress in Oceanography*, 71, 379–401, <https://doi.org/https://doi.org/10.1016/j.pocean.2006.09.006>, structure and function of contemporary food webs on Arctic shelves: a pan-Arctic comparison, 2006.
- 570 Moore, G. W. K., Schweiger, A., Zhang, J., and Steele, M.: *Spatiotemporal Variability of Sea Ice in the Arctic’s Last Ice Area*, *Geophysical Research Letters*, 46, 11 237–11 243, <https://doi.org/https://doi.org/10.1029/2019GL083722>, 2019.
- Moore, G. W. K., Howell, S. E. L., Brady, M., Xu, X., and McNeil, K.: *Anomalous collapses of Nares Strait ice arches leads to enhanced export of Arctic sea ice*, *Nat. Commun.*, 12, 1, 2021.
- Morisset, S.: *Canadian Coast Guard Ship Amundsen Thermosalinograph Data QA/QC Report*, *Processing report*, *Amundsen Science*, 1045
- 575 Avenue de la Médecine, Pavillon Alexandre-Vachon, Local 3432, Université Laval, Québec, QC, G1V 0A6, Canada, 2021.



- Mudryk, L. R., Derksen, C., Howell, S., Laliberté, F., Thackeray, C., Sospedra-Alfonso, R., Vionnet, V., Kushner, P. J., and Brown, R.: Canadian snow and sea ice: historical trends and projections, *The Cryosphere*, 12, 1157–1176, <https://doi.org/10.5194/tc-12-1157-2018>, 2018.
- Nadaï, G., Nöthig, E.-M., Fortier, L., and Lalande, C.: Early snowmelt and sea ice breakup enhance algal export in the Beaufort Sea, *Progress in Oceanography*, 190, 102479, <https://doi.org/https://doi.org/10.1016/j.pocean.2020.102479>, 2021.
- New, A. L., Smeed, D. A., Czaja, A., Blaker, A. T., Mecking, J. V., Mathews, J. P., and Sanchez-Franks, A.: Labrador Slope Water connects the subarctic with the Gulf Stream, *Environmental Research Letters*, 16, 084019, <https://doi.org/10.1088/1748-9326/ac1293>, 2021.
- Nghiem, S. V., Rigor, I. G., Perovich, D. K., Clemente-Colón, P., Weatherly, J. W., and Neumann, G.: Rapid reduction of Arctic perennial sea ice, *Geophysical Research Letters*, 34, <https://doi.org/https://doi.org/10.1029/2007GL031138>, 2007.
- 585 Niemi, A., Ferguson, S., Hedges, K., Melling, H., Michel, C., Ayles, B., Azetsu-Scott, K., Coupel, P., Deslauriers, D., Devred, E., Doniol-Valcroze, T., Dunmall, K., Eert, J., Galbraith, P., Geoffroy, M., Gilchrist, G., Hennin, H., Howland, K., Kendall, M., and Zimmerman, S.: State of Canada's Arctic Seas, *Canadian Technical Report of Fisheries and Aquatic Sciences* 3344, <https://doi.org/10.13140/RG.2.2.26859.16162>, 2020.
- Ogi, M., Rigor, I. G., McPhee, M. G., and Wallace, J. M.: Summer retreat of Arctic sea ice: Role of summer winds, *Geophysical Research Letters*, 35, <https://doi.org/https://doi.org/10.1029/2008GL035672>, 2008.
- 590 Peace, A. L., Dempsey, E. D., Schiffer, C., Welford, J. K., McCaffrey, K. J. W., Imber, J., and Phethean, J. J. J.: Evidence for Basement Reactivation during the Opening of the Labrador Sea from the Makkovik Province, Labrador, Canada: Insights from Field Data and Numerical Models, *Geosciences*, 8, <https://doi.org/10.3390/geosciences8080308>, 2018.
- Pizzolato, L., Howell, S. E. L., Derksen, C., Dawson, J., and Copland, L.: Changing sea ice conditions and marine transportation activity in Canadian Arctic waters between 1990 and 2012, *Clim. Change*, 123, 161–173, 2014.
- 595 Punshon, S., Azetsu-Scott, K., and Lee, C. M.: On the distribution of dissolved methane in Davis Strait, North Atlantic Ocean, *Marine Chemistry*, 161, 20–25, <https://doi.org/https://doi.org/10.1016/j.marchem.2014.02.004>, 2014.
- Ridenour, N., Straneo, F., Holte, J., Gratton, Y., Myers, P., and Barber, D.: Hudson Strait Inflow: Structure and Variability, *Journal of Geophysical Research: Oceans*, 126, <https://doi.org/10.1029/2020JC017089>, 2021.
- 600 Rohli, R. V. and Li, C.: *Weather Effects on the Coastal Ocean*, pp. 399–413, Springer International Publishing, Cham, https://doi.org/10.1007/978-3-030-73093-2_40, 2021.
- Science, A.: AVOS Meteorological Data collected by the CCGS Amundsen in the Canadian Arctic. Arcticnet Inc., <https://doi.org/10.5884/12518>, 2021a.
- Science, A.: CTD-Rosette data collected by the CCGS Amundsen in the Canadian Arctic. Arcticnet Inc., Québec, Canada., <https://doi.org/10.5884/12713>, 2021b.
- 605 Science, A.: TSG data collected by the CCGS Amundsen in the Canadian Arctic., <https://doi.org/10.5884/12715>, 2021c.
- Science, A.: Data Access - Amundsen Science, <https://amundsenscience.com/data/data-access/>, 2023.
- Serreze, M. C., Barrett, A. P., Stroeve, J. C., Kindig, D. N., and Holland, M. M.: The emergence of surface-based Arctic amplification, *The Cryosphere*, 3, 11–19, <https://doi.org/10.5194/tc-3-11-2009>, 2009.
- 610 Simpson, K. G., Tremblay, J.-e., Gratton, Y., and Price, N. M.: An annual study of inorganic and organic nitrogen and phosphorus and silicic acid in the southeastern Beaufort Sea, *Journal of Geophysical Research: Oceans*, 113, <https://doi.org/https://doi.org/10.1029/2007JC004462>, 2008.



- Straneo, F. and Saucier, F.: *The outflow from Hudson Strait and its contribution to the Labrador Current, Deep-Sea Research Part I: Oceanographic Research Papers*, 55, <https://doi.org/10.1016/j.dsr.2008.03.012>, 2008.
- 615 Tang, C. C., Ross, C. K., Yao, T., Petrie, B., DeTracey, B. M., and Dunlap, E.: *The circulation, water masses and sea-ice of Baffin Bay, Progress in Oceanography*, 63, 183–228, <https://doi.org/https://doi.org/10.1016/j.pocean.2004.09.005>, 2004.
- Untersteiner, N., Thorndike, A., Rothrock, D., and Hunkins, K.: *AIDJEX revisited: A look back at the U.S.-Canadian Arctic Ice Dynamics Joint Experiment 1970-78, ARCTIC*, 60, <https://doi.org/10.14430/arctic233>, 2009.
- Wareham, V. E. and Edinger, E. N.: *Distribution of deep-sea corals in the Newfoundland and Labrador region, Northwest Atlantic Ocean, Bulletin of marine science*, 81, 289–313, 2007.
- 620 Weatherhead, E., Gearheard, S., and Barry, R.: *Changes in weather persistence: Insight from Inuit knowledge, Global Environmental Change*, 20, 523–528, <https://doi.org/https://doi.org/10.1016/j.gloenvcha.2010.02.002>, governance, *Complexity and Resilience*, 2010.
- Williams, W. J. and Carmack, E. C.: *Combined effect of wind-forcing and isobath divergence on upwelling at Cape Bathurst, Beaufort Sea, Journal of Marine Research*, 66, 645–663, <https://doi.org/doi:10.1357/002224008787536808>, 2008.
- 625 Yang, Q., Dixon, T. H., Myers, P. G., Bonin, J., Chambers, D., van den Broeke, M. R., Ribergaard, M. H., and Mortensen, J.: *Recent increases in Arctic freshwater flux affects Labrador Sea convection and Atlantic overturning circulation, Nat. Commun.*, 7, 10 525, 2016.
- Yashayaev, I. and Seidov, D.: *The role of the Atlantic Water in multidecadal ocean variability in the Nordic and Barents Seas, Progress in Oceanography*, 132, 68–127, <https://doi.org/https://doi.org/10.1016/j.pocean.2014.11.009>, *oceanography of the Arctic and North Atlantic Basins*, 2015.
- 630 Zweng, M. M. and Münchow, A.: *Warming and freshening of Baffin Bay, 1916–2003, Journal of Geophysical Research: Oceans*, 111, <https://doi.org/https://doi.org/10.1029/2005JC003093>, 2006.